Consolidated verification report

AVNIR-2

	nom *fonction* *société*	*date* *signature*
Prepared by	Sébastien Saunier EOQC project manager GAEL Consultant **With contribution of ESA Prime Investigators.**	
Checked by	Yoelma Rodriguez EOQC engineer GAEL Consultant	
Authorized by	Christophe DEMANGE *Director* Gael Consultant	
Approved by	Philippe GORYL *project manager* ESA - ESRIN	

DISTRIBUTION LIST

GAEL	External	
S. SAUNIER	P. GORYL	ESA-ESRIN
Y. RODRIGUEZ	P. GRIMONT	ESA-ESRIN
A. MAMBIMBA	M. BOUVET	ESA-ESTEC
	F. VIALLEFONT	ONERA
	R. SANTER	LISE
	G. CHANDER	SAIC-EROS-USGS

DOCUMENT CHANGE LOG

Edition	Date	Comments	Author
0.1	20/10/2006	Creation of this document	S. Saunier
0.2	08/11/2006	Integration of contributions from ESA Prime Investigators	S. Saunier
0.3	15/11/2006	Review meeting with Philippe Goryl Marc Bouvet – comment on radiometry	S. Saunier
1.0	23/11/2006	Review meeting with Philippe Goryl	S. Saunier

TABLE OF CONTENT

LIST OF FIGURES

LIST OF TABLES

1 INTRODUCTION

1.1 Purpose

Purpose of this document is to report to ESA consolidated results collected during ALOS / AVNIR-2 data verification.

1.2 Document plan

- Chapter 1 Introduction and results summary,
- Chapter 2 Proposed some comments on product format,
- Chapter 3 Presents results from product geometry accuracy; absolute location, relative location, interband alignment,
- Chapter 4 Presents results on image quality, especially from modulation transfer function computation,
- Chapter 5 Presents results from activities regarding radiometric relative and absolute calibration accuracy.

1.3 Applicable documents

A-1	Contract - AMALFI Multi-Mission Facility *19284/06/I-LG* *14 February 2006* *ESA-ESRIN*

1.4 Reference document

R-1	GAEL-P224-DOC-003	*ALOS optical data verification* *Verification and Implementation Plan* Issue 1, Revision 3 – March 16th, 2006 GAEL Consultant
R-2	*NEB 00016*	ALOS/AVNIR-2 Level 1 product format description *Rev G - August, 2005* *JAXA*

1.5 Summary

This document reports results from 'in depth assessment' phase as part of ESA contribution to ALOS / AVNIR-2 calibration / validation activities. Main outputs of this technical study are summarized just here after.

The first validation activity has been focused on product format. The AVNIR-2 product processed into CEOS format complies with format specification document such as defined by JAXA. Improvements could be done in the fields of product accessibility through publication of documentation.

The second validation activity is the assessment of AVNIR-2 1B2 products geometric quality. This task has been performed according three validation items; band to band registration, relative geo location and absolute geo location. First item demonstrates that target accuracy is achieved and band-to-band registration remains mainly below 0.5 pixel. We observed some inconsistencies (between 0.5 and 1 pixel) with results into which band number 4 is involved, this issue shall be confirmed on more dataset and test play back after processing chain evolution.

The relative scene geo-location results tell us capability of AVNIR-2 scenes to be used as time series; it necessitates good geometric co registered image pair without taking ground control point for map projection procedure. We observed that shift between the both scenes is about 370 m (RMS), so that target accuracy is not reached.

The absolute scene geo-location results confirm previous results; a persistent bias remains from 500 m up to 1800 m for observation performed with high pointing angles (41.5 °). Study demonstrates that accuracy has improved over time.

Shift occurs mainly along the north direction; its magnitude strongly depends on acquisition data and pointing angle. Shift along the Eastern one remains more stable. We note some improvements for product processed with the version of processing chain dated of August 06' beginning.

For one scene, we investigate more in-depth inner geometry quality. We conclude that geo location shift is mainly due to a platform translation according to roll and yaw axis (satellite reference frame). When geo location is corrected from this linear transformation, geo location accuracy reaches goal of 60 m in Eastern direction and 20 m in northing direction. Again, due to acquisition with not null pointing angle, the contribution of transformation due to scale change is observed, its contribution remains acceptable. Transformation due to rotation has not been observed, it presents a good point.

Coefficient given for polynomial transformation should be refined and the use of rational polynomial coefficients may be more suitable for the achievement of a good accuracy.

The third validation activity has been focused on image quality through visual inspection and the estimate of Modulation Transfer Function. At the end of visual inspection we concluded that image quality looks good, good sharpness of image edge, noise is reduced over uniform area. Some image artifacts has however been observed; residual striping along image row and missing data, probably due to problem when using of satellite data relay system. Saturation occurs occasionally on image data, this is due to the use of wrong gain setting during data acquisition; situation should be recovered with the improvement of on board process dedicated to compute the best gain state according geographical region.

ONERA Team, MTF estimate, demonstrates that AVNIR-2 has a good capability to discern ground features, and results are mainly within pre launch specifications. In the future, validation should be played back on a new dataset, especially for band 4 because of image saturation.

The fourth validation activity has addressed issues regarding radiometric calibration with in the one hand; assessment regarding band to band calibration stability and radiometric calibration stability has brought and in the other hand sensor inter comparison; ALOS AVNIR-2 / Landsat TM and ALOS AVNIR-2 / ENVISAT MERIS.

Band to band calibration and radiometric calibration stability validation items underlined a good stability of radiometric calibration,; over three months of time series data observation, variation doesn't exceed 5 %. Inconsistent results have been observed for one product on band number 4, it is more likely due to atmospheric effect and water vapor content at the date of observation shall be checked for confirming.

Regarding sensor intercomparison between AVNIR-2 with Landsat TM at TOA level, saturation on AVNIR-2 band 3 has made difficult a direct comparison with TM. However, results for the other bands are summarized as follow:

- AVNIR-2 band 1 TOA radiances are 4% lower than TM ones.
- AVNIR-2 band 2 TOA radiances are 3.7% upper than TM ones.
- AVNIR-2 band 4 TOA radiances are 1.81% upper than TM ones.

The average percent differences in radiance estimates obtained from the ALOS AVNIR-2 agree with those from the L5 TM to within 5%. One keep in mind that these values have been tested at one date, over a somewhat peculiar target (Libya) – more dates and sites must be tested to develop more robust relationships. It is difficult to interpret these results directly in terms of calibration differences between LANDSAT TM and AVNIR-2 because the two sensors did not acquire data in bands having identical spectral responses and under identical viewing and illumination geometries.

Sensor intercomparison procedure has been based on reference data from ENVISAT/MERIS-AATSR and PARASOL as well. This assessment has been conducted though a direct comparison of TOA reflectance and a simulation of AVNIR-2 signal using exogenous data.

Results from the direct comparison method are difficult to interpret because of difference in term of viewing and illumination geometry, acquisition date and spectral responses. At a first order, we observed a good agreement (20%) when comparing TOA from AVNIR-2 instrument and TOA from reference instrument.

Comparison with the simulation of AVNIR-2 signal gives similarities on the order of 6% except for band number 1 (11%). Blue band results magnified a strong variability. One explanation could be the use of approximate value regarding spacecraft and sun azimuth/ zenith angles.

2 PRODUCT FORMAT

This first chapter aims at listing some comments on product format and information embedded within it.

For information, products are processed into CEOS format, and external ASCII file ('summary.txt') is embedded with the product.

2.1 Encoding

A mixing between "little endian" and "big endian" encoding system reference is done for data belonging to AVNIR-2 product processed into CEOS format.

For instance, into the ALOS ancillary information files map projection, drift values (according X,Y and Z direction) are encoded as "little endian' (arch x86) whereas values belonging to quaternion fields are encoded as "big endian" " (arch sparc).

2.2 Radiometric transformation

Conversion from AVNIR-2 digital number to radiance values required knowledge of rescaling gain and offset. These values are provided with CEOS scene header record but not in the summary file. Major parts of end-user tools are not able to access into CEOS format, except for image data.

To rebuild a viewing geometry at the time of acquisition is required when computing cross calibration results.

AVNIR-2 product is proposing sun zenith and azimuth angles. No information is provided on satellite zenith and azimuth angles. High pointing angle of AVNIR-2 instrument makes the correspondence between satellite heading and satellite azimuth values not reliable anymore.

The only way for comparing two viewing geometry is to compute satellite zenith and azimuth angle at the AVNIR-2 scene centre. Doing this with product for which processing level is 1B2 can be constraints because time information is missing for such level. On the other side, due to stagger alignment of CCDs of AVNIR-2 raw geometry, image data from level 1B1 product may not be suitable for radiometric assessment purpose.

Band solar spectral irradiance values are not proposed with the standard L1B2 AVNIR-2 product as done with Landsat CEOS format.

2.3 Geometric transformation

During the calibration validation phase, the whole of AVNIR-2 products where processed using a geometric sampling step of 10 meter. As figure just here below depicts (fig. 1), for observations taken with an important pointing angle, the 10-meter resolution hypothesis is not reliable anymore. And when controlling product geo location, for an area observed with a 40 degree pointing angle with a product processing done on the basis of a 10 meter pixel resolution, it impacts negatively on final results.

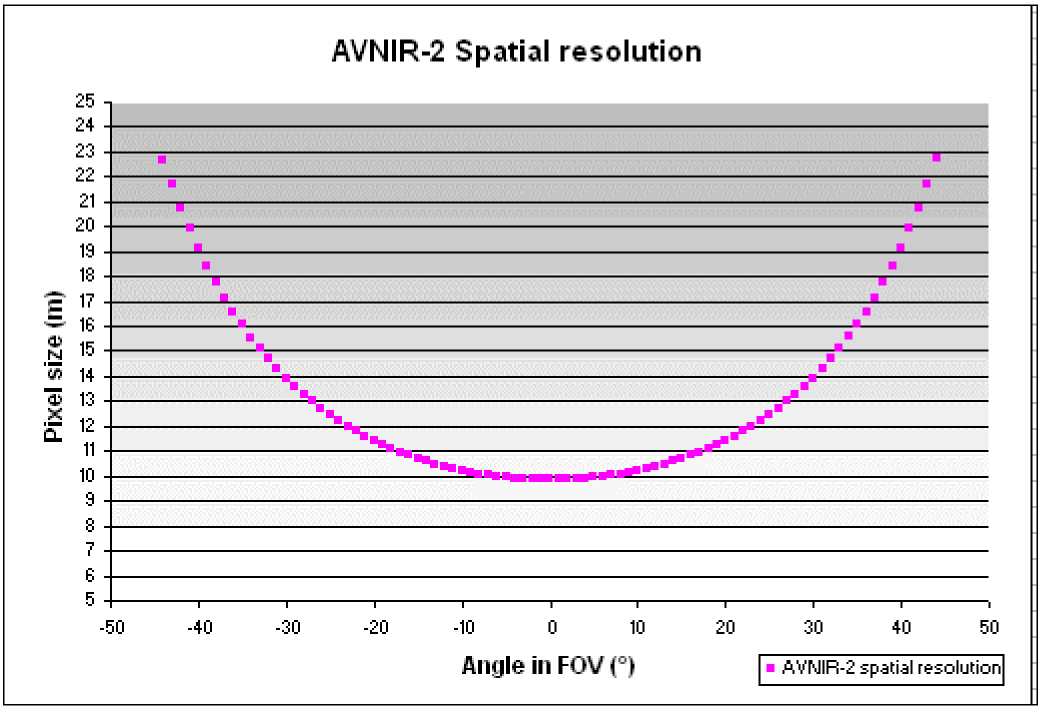

fig. 1 - AVNIR-2 spatial resolution.

A polynomial transformation for geo coding purpose is proposed with the both 1B1 and 1B2 levels. This transformation does not take into account vertical dimension. So that, computation based on this transformation is not rigorous and constraint for some validations / applications; especially when investigating on internal geometry of image data.

In addition, geographical coordinates of the scene can be retrieved from summary file. Following information is proposed:

```
Img_ImageSceneCenterLatitude="28.374"
Img_ImageSceneCenterLongitude="23.448"
Img_ImageSceneLeftTopLatitude="28.859"
Img_ImageSceneLeftTopLongitude="22.820"
Img_ImageSceneRightTopLatitude="28.493"
Img_ImageSceneRightTopLongitude="24.270"
Img_ImageSceneLeftBottomLatitude="28.251"
Img_ImageSceneLeftBottomLongitude="22.627"
Img_ImageSceneRightBottomLatitude="27.887"
Img_ImageSceneRightBottomLongitude="24.070"
```

One observes that values are given on the order of 10 e-3 degrees that leads to an accuracy of about 110 meters.

3 PRODUCT GEOMETRY

3.1 Absolute location accuracy

Purpose

Purpose of this validation item is the assessment of geodetic accuracy of PRISM / AVNIRS-2 L1B2R through the use of geo-referencing function. Main output of this task would be the location accuracies expressed in term of root mean square results. The mean displacement of product geo-location will be highlighted. The multi-temporal case will be a part of this validation item. Internal geometry control is performed using an alternative method depicted just here below.

Method

Method is semi -automatic; an operator sets Ground Control Points (GCP) manually on the working data. GCP geographical coordinates are matched with the ones belonging to the reference data. Operator adjusts the GCP location for ensuring the best matching between the both views.
In doing this, with at least 20 GCPs, model of acquisition is re build and compare to the reference model. Method leads to a statistical displacement results in term of easting and northing between the AVNIR-2 1B2 image and a corresponding reference one.
Internal geometry control is performed through the study of RMS results when removing image deformation; if RMS results remains stable whereas rotation effect has been estimated and subtracted, it means internal geometry of AVNIR-2 data is not contaminated with rotation effect.
Accurate internal geometry assessment requires viewing geometry and parallax effect estimate, especially with AVNIR-2 data observed with high pointing angle. For one dataset, 50 GCPs has been identified in order to statically estimate the parallax effect and proposed coherent results on internal image geometry for which parallax effect has been removed.

Team

GAEL Consultant

Working data

Following ALOS / AVNIR-2 dataset sample, acquired over La Crau target zone (4.875°, 43.513°) has been used for assessment on product geo location.

Observation date	Scene Id	Pointing angle	Path	Orbit data Precision	Attitude data Precision
15-juil-06	ALAV2A025142730	-21,5	317	Precision	OnSite Precision
21-juil-06	ALAV2A026022690	41,5	344	Precision	AOCS Precision
23-juil-06	ALAV2A026312710	21,5	331	Precision	OnSite Precision
14-août-06	ALAV2A029522700	34,3	338	Precision	OnSite Precision
30-août-06	ALAV2A031852730	-21,5	317	Precision	AOCS Precision

table 1 - Dataset used for assessment of product geo location accuracy.

Reference data

Reference dataset sample is a SPOT4 one. Data validation and geometric correction procedures using reference map have been performed at GAEL Consultant.

Results

Multi-temporal analysis

Firstly, we observed that RMS results is strongly varying according to acquisition date; around 495 m for observation dated of August, 30, RMS reaches 1780 m for observation dated of July, 21.

We notice that RMS results are correlated with pointing angle; the wider pointing angle, the greater RMS is. Products from observation with high and positive pointing angle give less accurate results than the ones observed with low and negative pointing angle.

Tendency regarding direction of the shift (X: Easting, Y: Northing) is not homogeneous along with acquisition date. For certain acquisition magnitude of the shift is more important according to Easting direction and for other ones the shift is more pronounced according to the Northing direction.

Actually, we observed that for product observed with positive pointing angle the shift according to Northing direction (RMSY) is systematically superior to the shift according the Eastern direction (RMSX). This situation is changing when considering observation with a negative pointing angle; RMSY result becomes inferior to 200m and RMSX result (592 m) are in mean superior to RMSX result (252.737 m) from data observed with positive pointing angle.

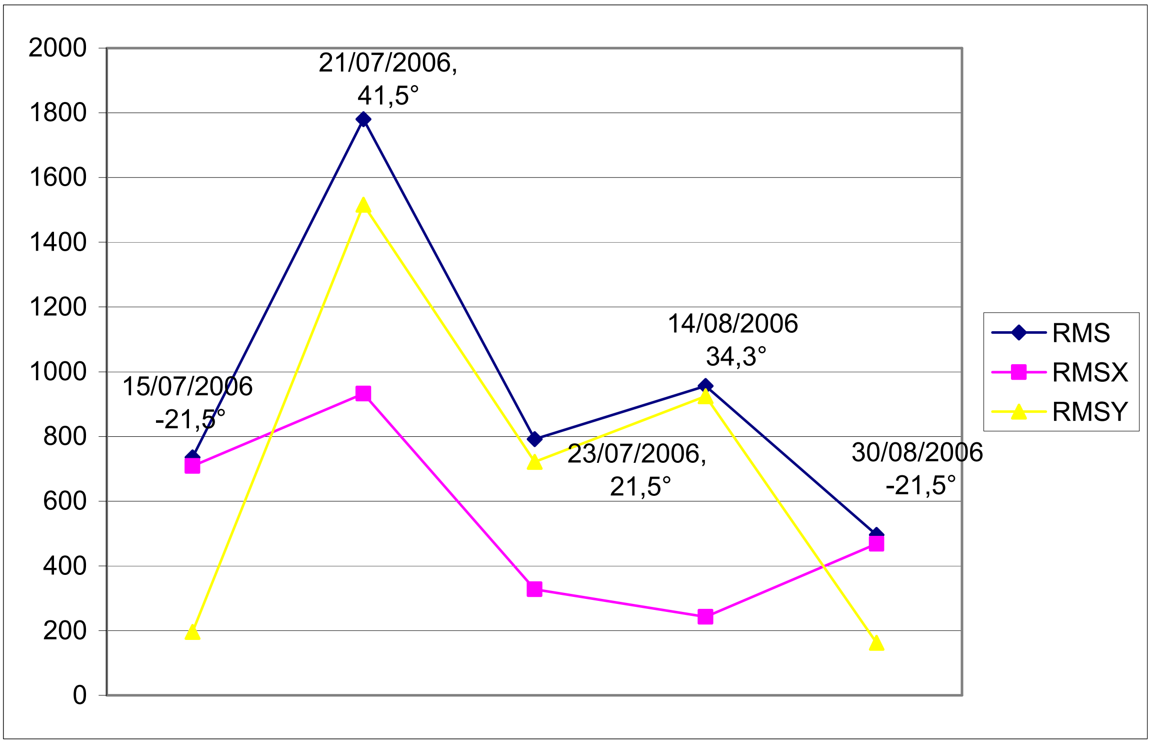

fig. 2 - RMS trends

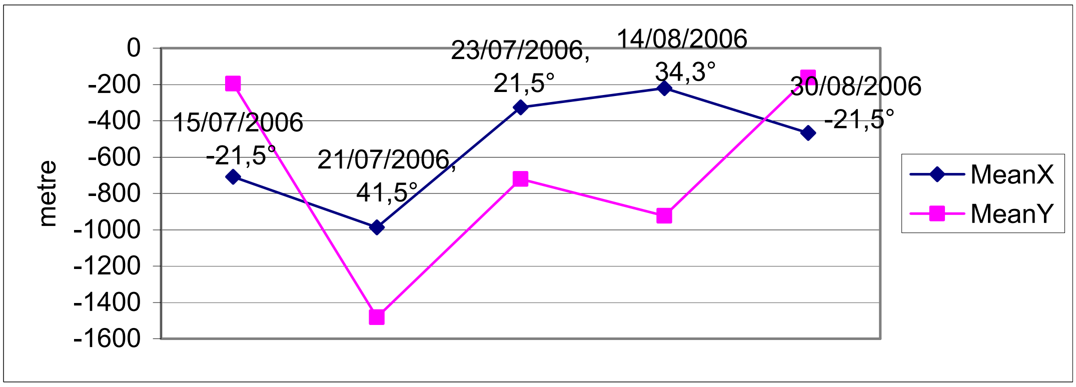

fig. 3 - Mean displacements trend.

The bad standard deviation results getting from product dated of August 14 is due to hazy atmospheric conditions that make difficult the identification of ground control point.

Except this observation, deviation along X-axis remains between 20 and 44 meter, and deviation along Y - axis does not exceed 11 meter.

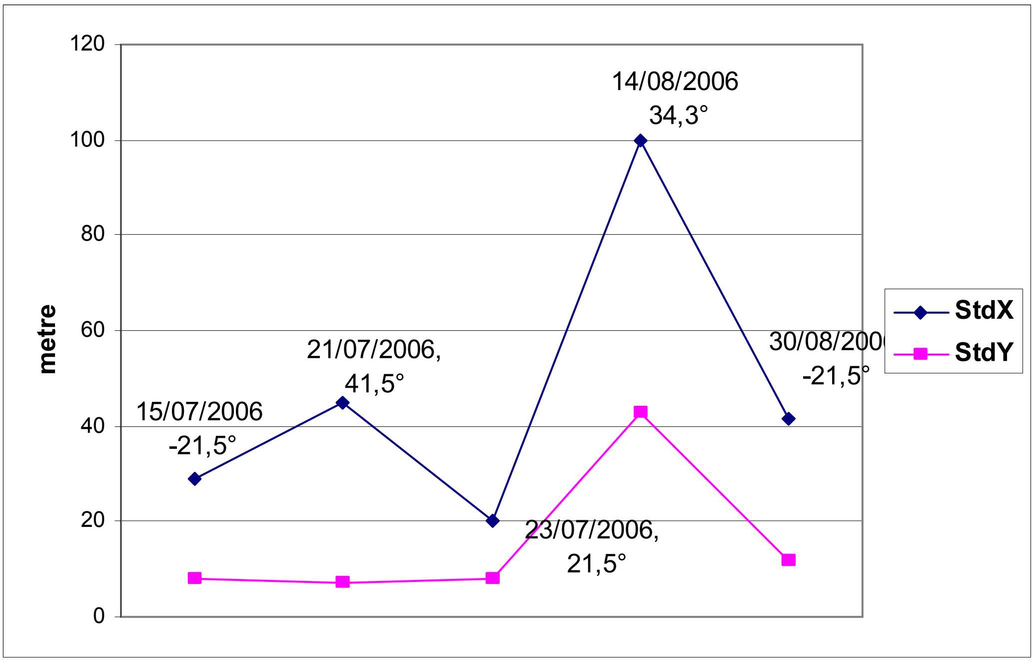

fig. 4 - Standard deviation trend.

Geometry control of AVNIR-2 observation dated of August, 30

When adding ground reference point for compensating some geometric transformation such translation; rotation and similitude, RMS results improve until the use of 3 GRPs.

We notice a dramatic improvement; when one GRP is used; error components regarding geo location shift is removed, it means 91% of global RMS error.

Using two ground reference points, geo location improved slightly and RMS reach 45.975 meter. In doing this image geometric model is corrected from rotation.

The use of three ground reference points does not improved product geo location. Remaining RMS is now essentially due to internal geometry error, parallax effect.

GCP number	0.GRP	1.GRP	2.GRP
Mean X	-716,2	-41,781	9,722
Mean Y	-189,997	14,510	-4,906
Mean	740,58	44,229	40,091
Std X	42,285	42,509	42,334
Std Y	14,077	14,078	14,246
Std	39,361	44,780	22,503
RMS X	717,269	59,605	43,436
RMS Y	188,253	20,217	15,067
RMS	741,64	62,940	45,975

table 2 - ALAV2A03625380 product; geo-location accuracy results.

GCP Number 54

Mean altitude 50 m.

Parallax effect

For 40% percent of ground control points, altitude is between 100 and 450 meters. It means error due to parallax is integrated within results. After correction using two-ground reference point, statistical analysis has been performed on ground control point's error results.

When matching error in dX direction (Easting) and altitude, we observed that the both variable are linearly dependant dX error on every GCP can be interpolated using linear transformation for which the slope is –0.38. Quality of interpolation maybe considered as good, since a confidence reaches 90%.

In addition,, when simulating parallax magnitude along altitude object for a given pointing angle (20 degree), we observed a same linear dependency; the slope is about -0.38.

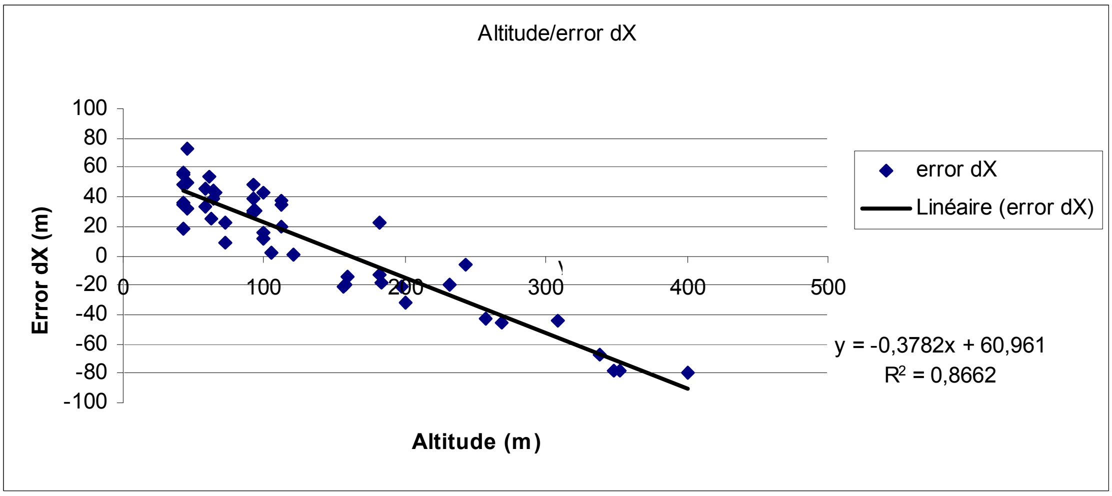

fig. 5 - Error dX along with altitude.

Correlation between error dY and altitude is less important (65% confidence) . So that; no correction will be applied to dY error results.

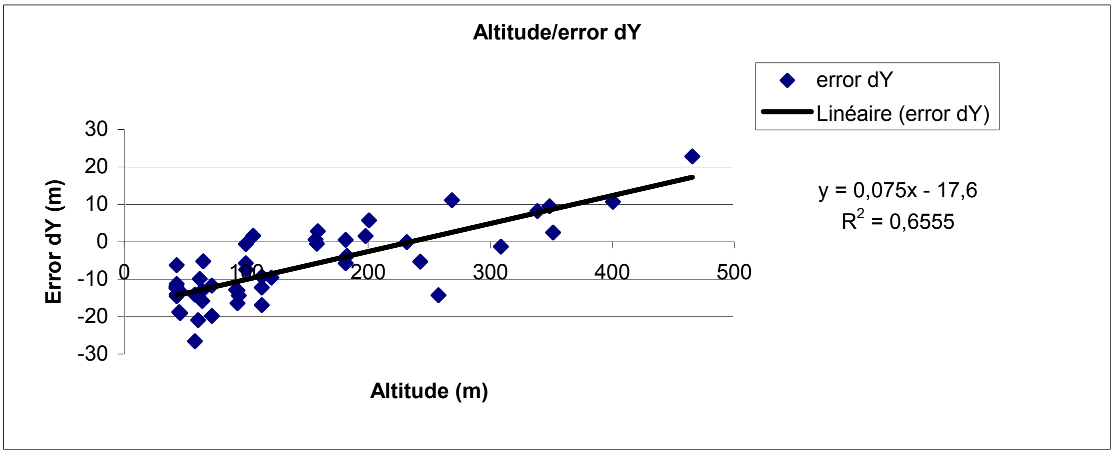

fig. 6 - Error dY along with altitude.

Final results

Synthesis

Final results are based on less ground control points. Points belonging to an altitude below 100 meters have been kept. It represents 60 % of total population.

GCP number	0.GRP	1.GRP	2.GRP	2GRP + parallax correction
Mean X	-716,2	-41,781	9,722	0,27
Mean Y	-190	14,510	-4,906	-7
Mean	740,58	44,229	40,091	17,240
Std X	42,285	42,509	42,334	14,250
Std Y	14,077	14,078	14,246	9,890
Std	39,361	44,780	22,503	6,870
RMS X	717,269	59,605	43,436	14,253
RMS Y	188,253	20,217	15,067	12,117
RMS	741,64	62,940	45,975	18,707

table 3 - ALAV2A03625380 product; geo-location accuracy results (with correction).

X tendency after correction

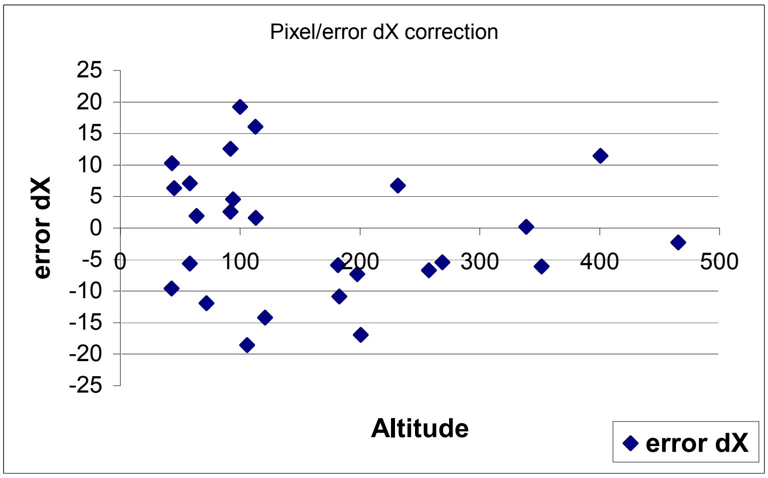

fig. 7 - Corrected error dX along with altitude.

Error vector Fields

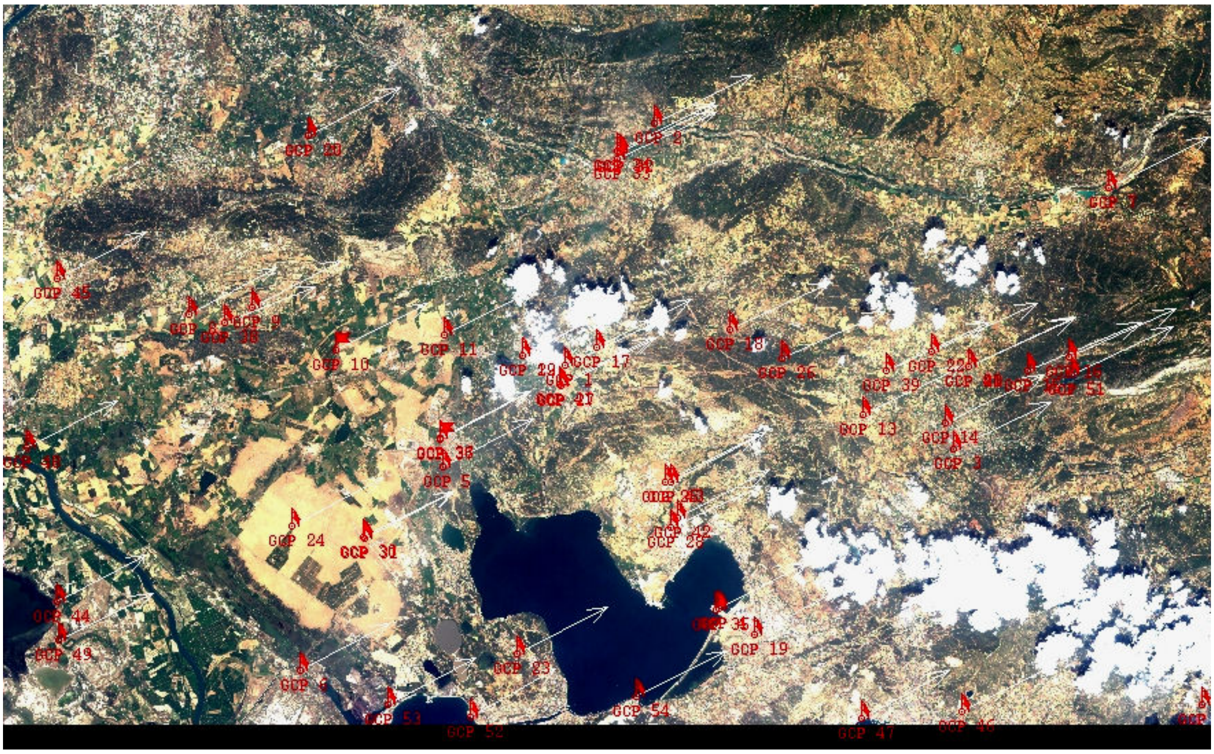

fig. 8 - ALAV2A03625380 product; error vector fields (x100) overlaid image data (no grp).

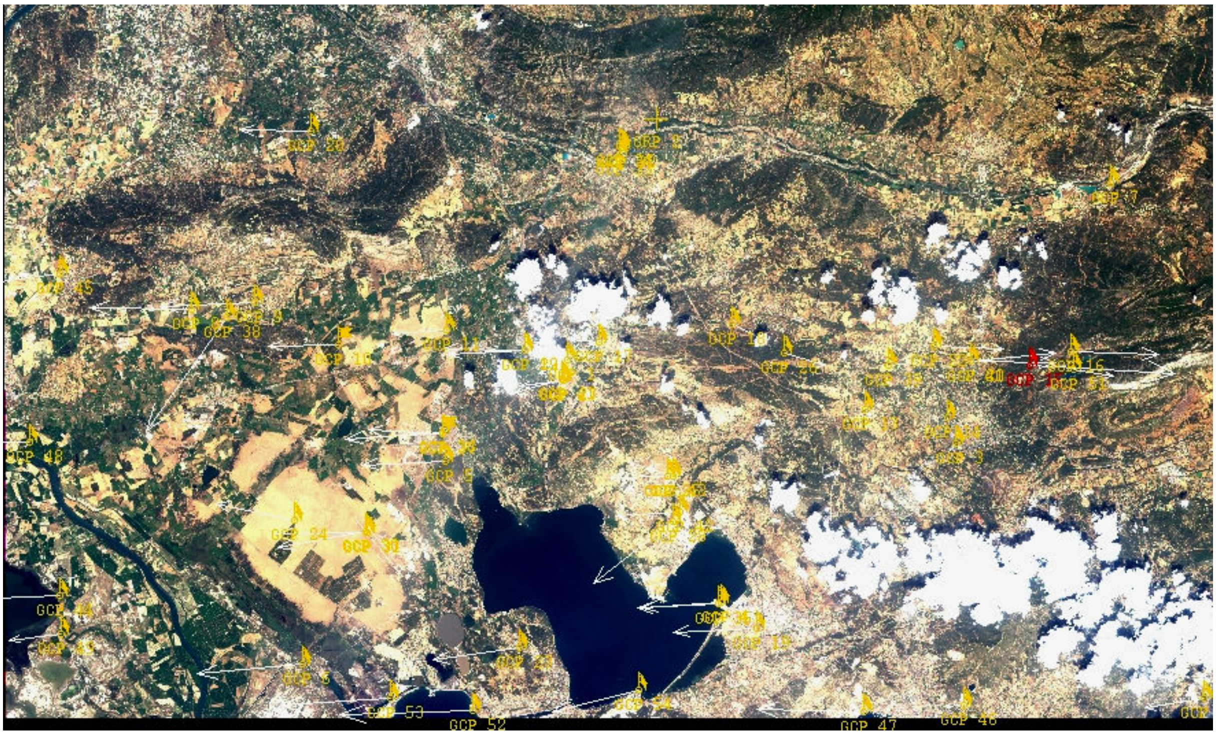

fig. 9 - ALAV2A03625380 product; error vector fields (x10) overlaid image data (one grp).

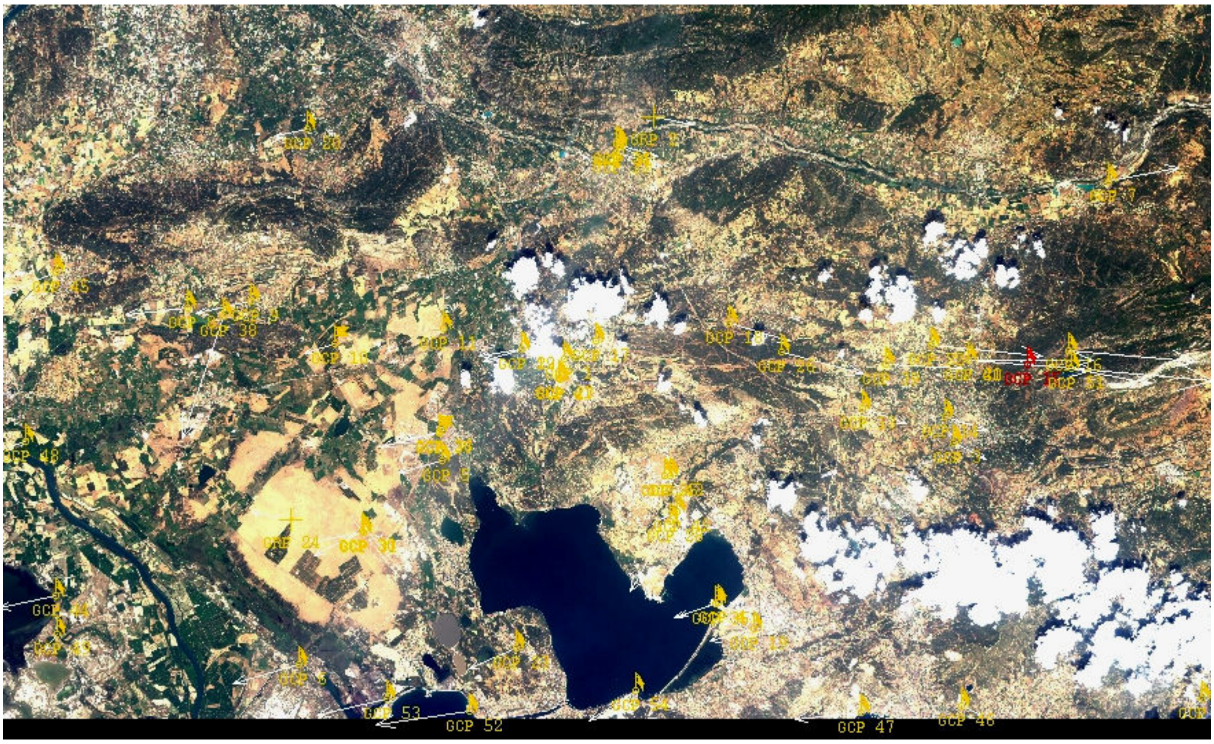

fig. 10 - ALAV2A03625380 product; error vector fields (x10) overlaid image data (two grps).

CE90 representation

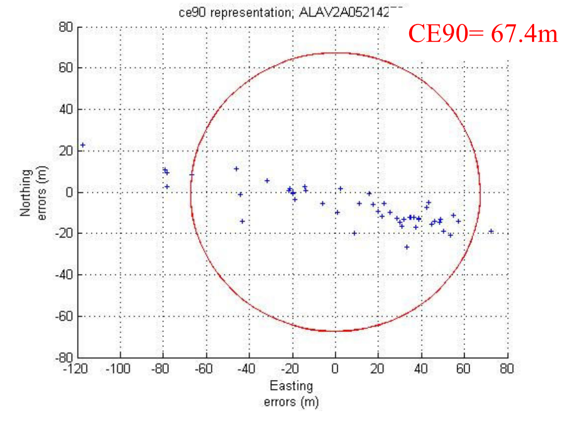

Without correction of X error

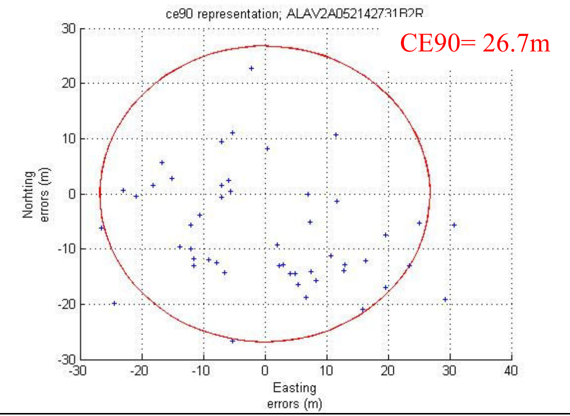

Without correction of X error

fig. 11 - CE90 graphic plots.

3.2 Relative registration

Purpose

The relative scene geo-location results tell us capability of AVNIR-2 scenes to be used as time series; it necessitates good geometric co registered image pair without taking ground control point for map projection procedure.

Method

Method used has been detailed with previous validation item.

Team

GAEL Consultant

Working data

Following ALOS / AVNIR-2 dataset sample, acquired over La Crau target zone (4.875°, 43.513°) has been used for band-to-band registration accuracy assessment.

Observation date	Scene Id	Pointing angle	Path	Orbit data Precision	Attitude data Precision
15-juil-06	ALAV2A025142730	-21,5	317	Precision	OnSite Precision
30-août-06	ALAV2A031852730	-21,5	317	Precision	AOCS Precision

table 4 - Dataset used for assessment of relative geo location accuracy.

Results

Mean X	Mean Y	Mean	Std dev X	std dev Y	Std dev	RMS X	RMS Y	RMS
-356,85	-98,71	370,3	13,697	6,974	13,177	357,113	98,956	370,6

table 5 - ALAV2A03625380/31852730 product; geo-location accuracy results.

We observed that shift between the both scenes is about 370 m (RMS), so that target accuracy is not reached

3.3 Band to band registration

Purpose

Purpose of the validation item is to check that AVNIR-2 channels of L1B2 product can be perfectly superimposed.

Method

Verification is performed through an automatic test for measuring the offset of all band pair. The method relies on correlation matrix algorithm. It allows interpolation in a reference band of an estimated in other bands.

Test is applied for data acquired over a dedicated test site. Actually, for results consistency, spectral difference between bands shall be minimized and computation shall be concentrated on a specific area.

For validating results from the automatic procedure, a manual procedure is added and results from the both method are compared. Finally, if results are consistent, displacements evaluated with automatic method are kept.

Team

GAEL Consultant

Working data

Following ALOS / AVNIR-2 dataset sample, acquired over La Crau target zone (4.875°, 43.513°) has been used for band-to-band registration accuracy assessment.

Observation date	Scene Id	Pointing angle	Path	Orbit data Precision	Attitude data Precision
15-juil-06	ALAV2A025142730	-21,5	317	Precision	OnSite Precision
30-août-06	ALAV2A031852730	-21,5	317	Precision	AOCS Precision

table 6 - Dataset used for assessment on band-to-band registration accuracy.

Results

Results are expressed in pixel unit. Accuracy of measurement is 10%.

	band1		band2		band3		band4	
	x	y	x	y	x	y	x	y
band1	x	x	0,47	0,47	0,54	0,38	0,94	0,79
band2	0,47	0,47	x	x	0,58	0,42	0,77	0,62
band3	0,54	0,38	0,58	0,42	x	x	0,81	0,59
band4	0,94	0,79	0,77	0,62	0,81	0,59	x	x

table 7 - ALAV2A025142730 product; Band to band registration results.

	band1		band2		band3		band4	
	x	y	x	y	x	y	x	y
band1	x	x	0,43	0,44	0,51	0,35	0,87	0,75
band2	0,43	0,44	x	x	0,53	0,39	0,72	0,57
band3	0,51	0,35	0,53	0,39	x	x	0,71	0,54
band4	0,87	0,75	0,72	0,57	0,71	0,54	x	x

table 8 - ALAV2A031852730 product; Band to band registration results.

4 PRODUCT IMAGE QUALITY

4.1 Visual comparison between AVNIR-2 data and SPOT4 data

Interband

SPOT4 Data - panchromatic band	AVNIR-2 Data - band 1 2 3 composition
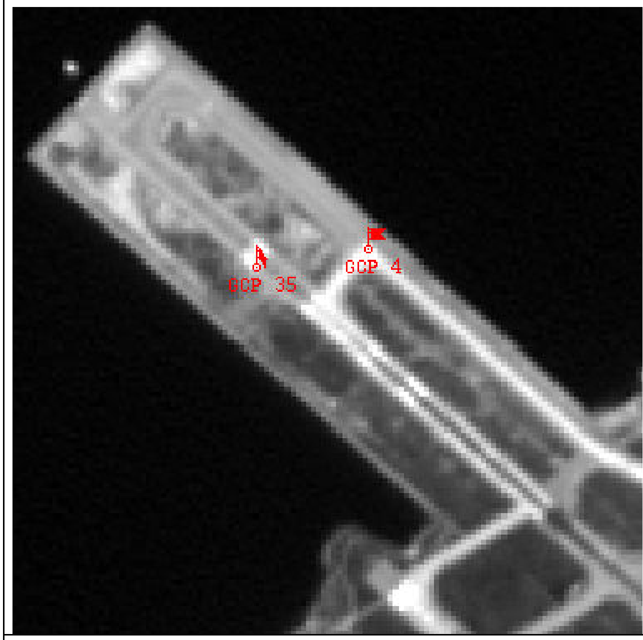	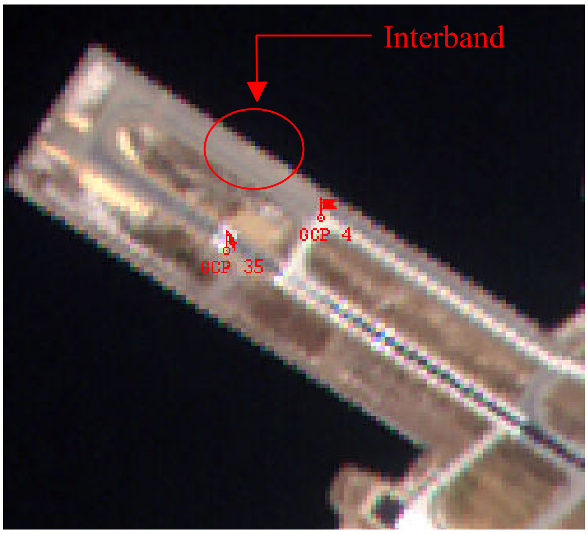
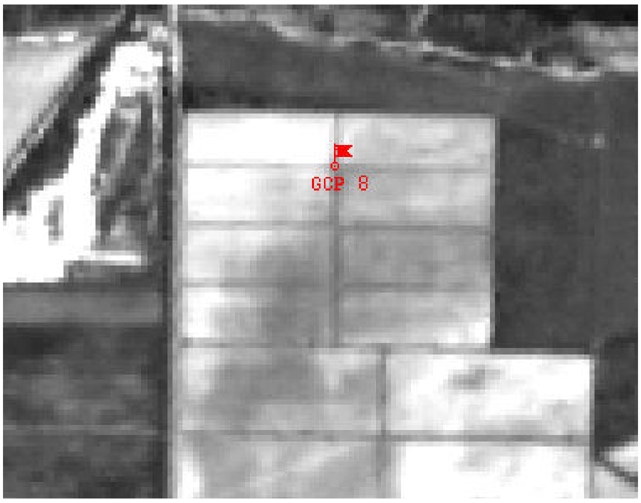	

Missing data

Anomaly is observed for the level1B1 and level 1B2 product as well . This is more likely due to data transmission lost.

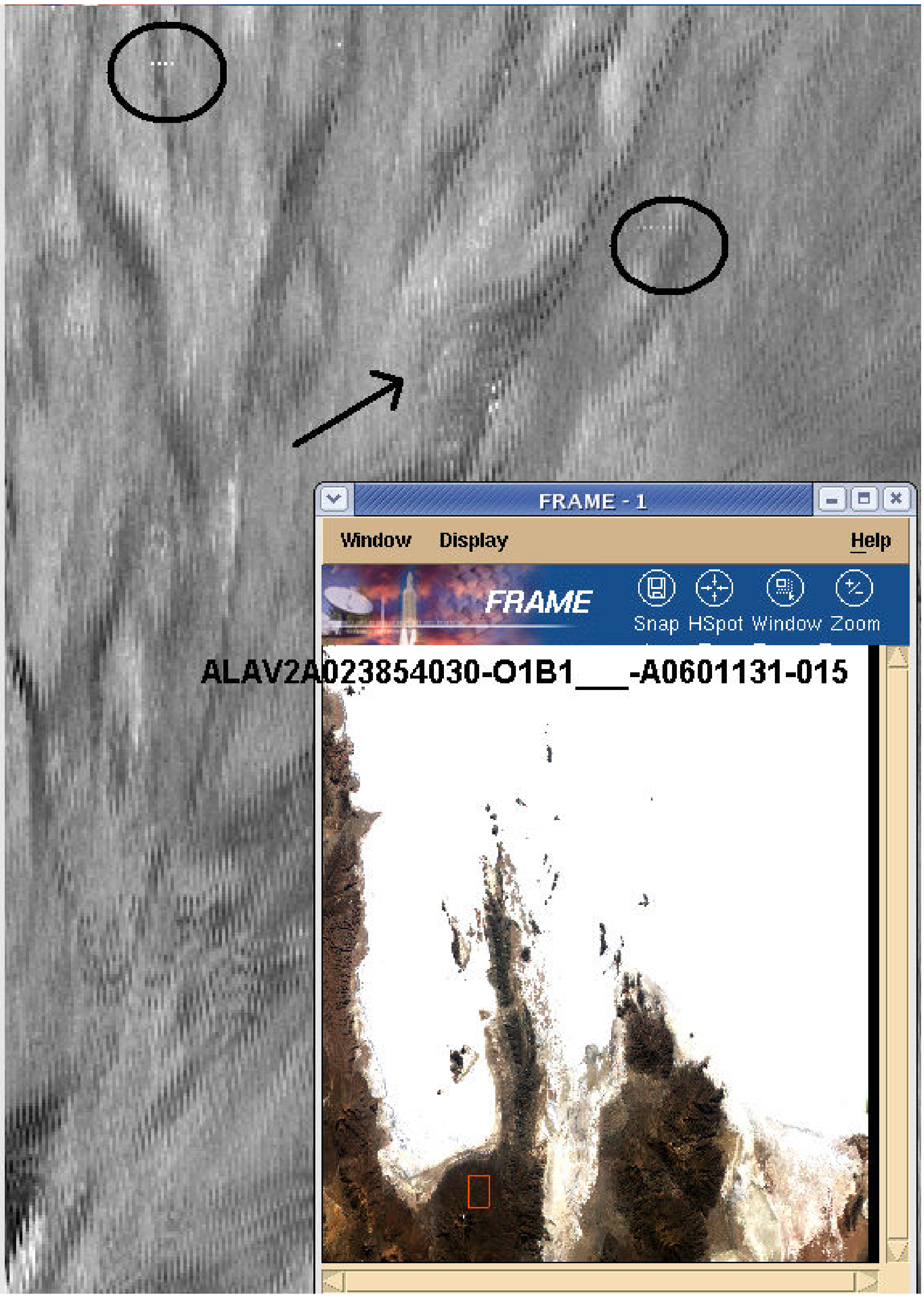

fig. 12 - Missing data, 1B1 product.

fig. 13 - Missing data, 1B2 product.

4.2 Modulation transfer function results

<u>Purpose</u>

To evaluate and quantify capability of AVNIR-2 instrument discern ground features.

Method

•LR/HR method requires similar radiometries between Low Resolution (LR° and High Resolution (HR) spectral bands

AVNIR MTF assessment has been performed for Band 1 •Band 2 •Band 3.

Gael Consultant was in charge of building the image row without resampling (translation only); transformation of 1B1 product into row image geometry.

AVNIR Image is splitted into small images 256 pixels wide, following curves correspond to an average over the small images results (fig. 14).

Team

Francoise Viallefont, Dominique Leger (ONERA).

Working data

Following ALOS / AVNIR-2 dataset sample, acquired over La Crau target zone (4.875°, 43.513°) has been used for band-to-band registration accuracy assessment.

Observation date	Scene Id	Pointing angle	Path	Orbit data Precision	Attitude data Precision
15-juil-06	ALAV2A025142730	-21,5	317	Precision	OnSite Precision
30-août-06	ALAV2A031852730	-21,5	317	Precision	AOCS Precision

table 9 - Dataset used for assessment on band-to-band registration accuracy.

Results

Results are listed in table 10. They are globally in agreement with the pre-flight measurements and within the specifications (marginally for band 1 in along-track direction). Due to the measurement method and saturation observed on image band number 4, no MTF assessment has been performed.

MTF at Nyquist frequency	Band 1	Band 2	Band 3
CT MTF (x)	0.51	0.50	0.48
AT MTF (y)	0.24	0.30	0.32
CT MTF (pre-flight)	0.54	0.51	0.48
AT MTF (pre-flight)	0.35	0.34	0.36
Specification	>0.25	>0.25	>0.25

table 10 - AVNIR-2; MTF at Nyquist frequency.

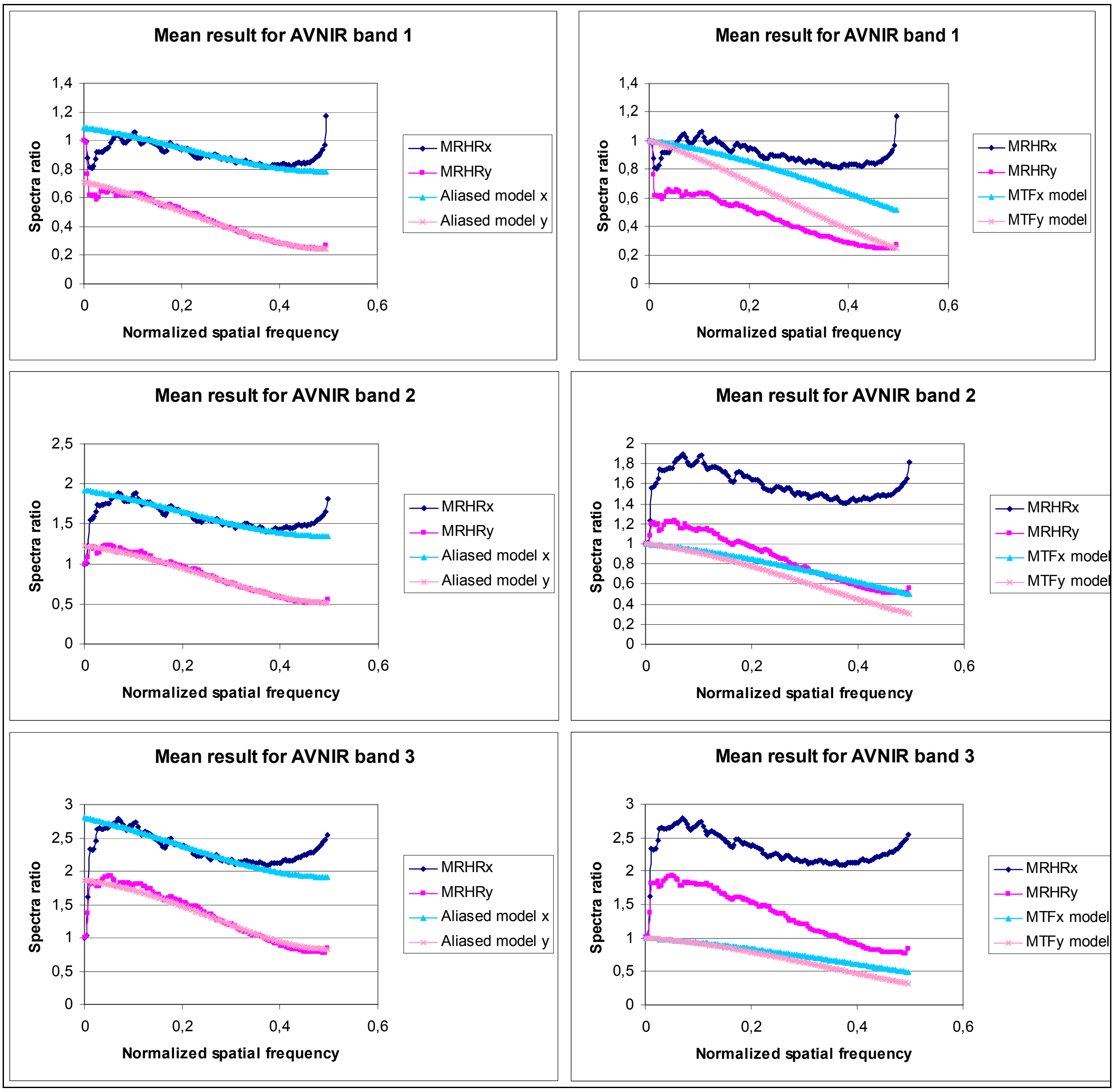

fig. 14 - LR / HR graphic plots.

5 PRODUCT RADIOMETRIC CALIBRATION

5.1 Assessment of the band to band radiometric stability

Purpose

The purpose of this verification is to check that band-to-band ratio time series remain constant over time.

Method

This method relies on the geometric co-registration procedure for the whole of dataset sample.

Looking into band ratio time series help removing the first order dependency of the TOA reflectance on the cosine of the solar zenith angle and the viewing zenith angle. Assuming that the surface properties of the Libyan site are spatially homogeneous and the TOA reflectance is stable over time, to a first approximation, this method enables identification of important (larger than about 10%) calibration changes/drift on a band to band basis.
Several regions of interest are disseminated over each scene. The regions are located on the area for which the overlapping between consecutive scenes is the most important (fig. 15).

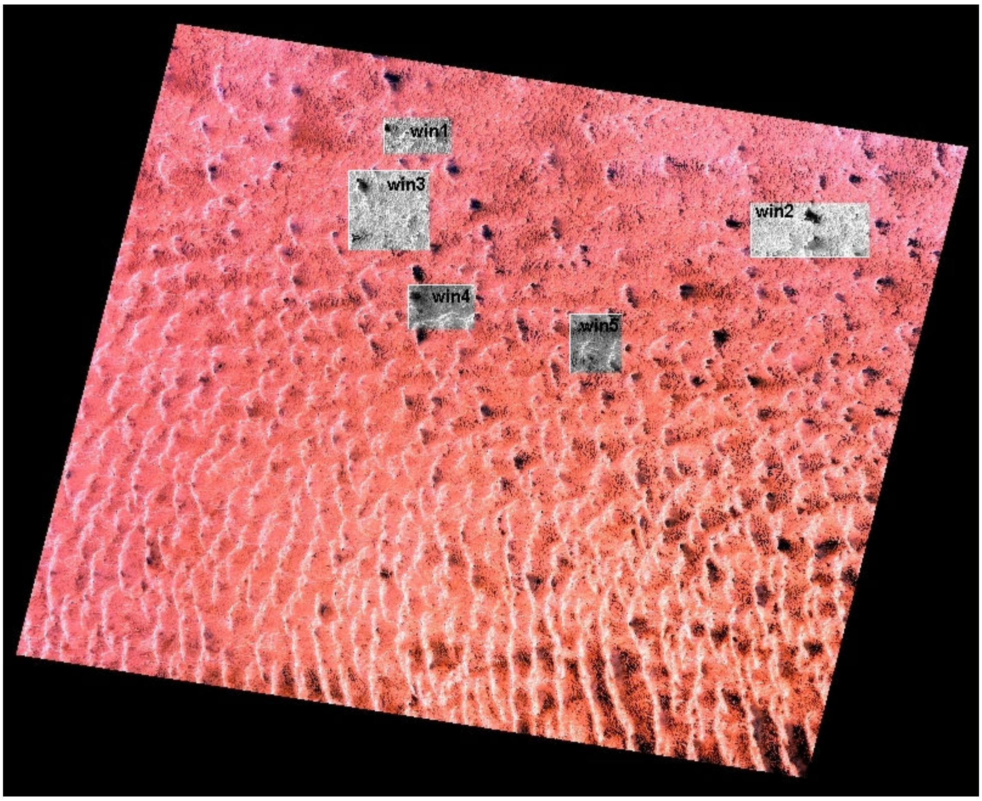

fig. 15 - Area of interest used for verification of band to band calibration stability.

Team

Sebastien Saunier (GAEL Consultant), Richard Santer (LISE), Marc Bouver (ESA / ESTEC)

Working data

Observation date	Scene Id	Pointing angle	DOY
16-mai-06	ALAV2A016383020	0	136
31-mai-06	ALAV2A018573000	34,3	151
24-juin-06	ALAV2A022073010	21,5	175
26-août-06	ALAV2A031263000	21,5	238

table 11 - Dataset used for verification of band to band calibration stability.

Results

The results show that a band ratio stability is observed until DOY 175. After this date, ratios involving band 4 show significant differences from the other band ratios.

Whereas the standard deviation of ratio for the 4 acquisitions remains below 0.6% for combination involving band number 1,2,3, the situation becomes different for ratios based on band 4.

In this case, the ratio standard deviation is above 1% and reaches 9.06% for the band ratio between band 2 and 4.

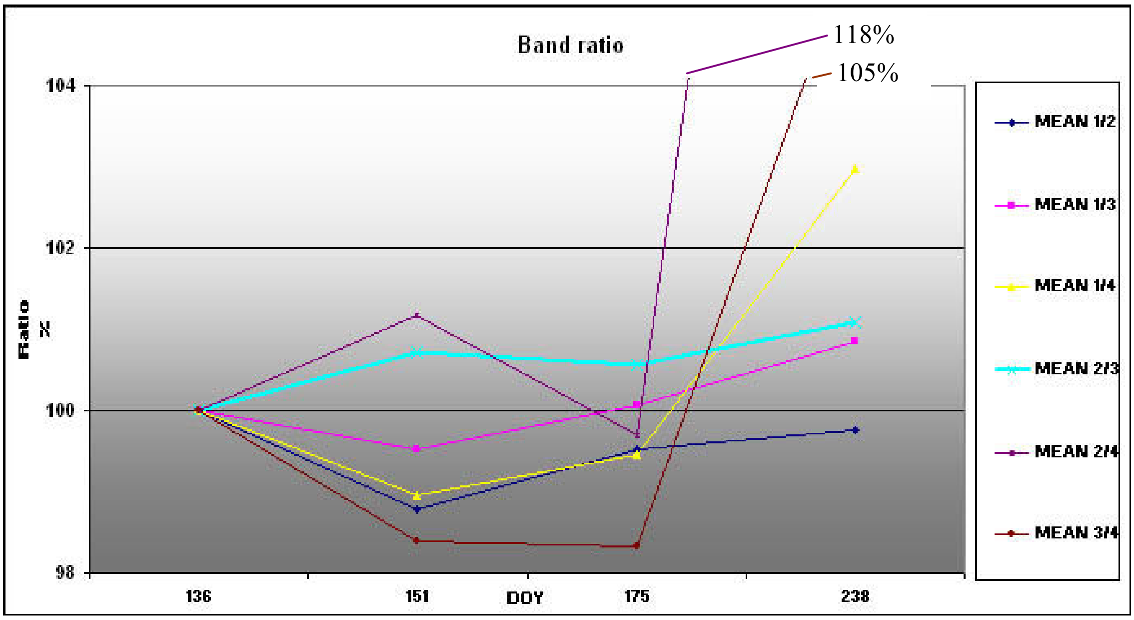

The band ratios remain stable until DOY 175 and become abnormal for the observation on the DOY238. This discrepancy between DOY238 observation and the previous ones is not due to pointing angle since it is the same as DOY 175 (21.5°).

A similar analysis including more data acquisitions should be carried out before drawing any final conclusions.

5.2 Assessment of radiometric calibration stability

Purpose

Purpose of this validation item is to monitor stability of AVNIR-2 radiometric calibration.

Method

We use a multitemporal analysis of the Top Of Atmosphere (TOA) reflectance over a Libyan target. Such analysis of TOA reflectance time series relies on the assumption that:

- the atmospheric and surface bidirectionality can be neglected and the TOA reflectance distribution is Lambertian
- the TOA reflectance is stable over time for the temporal window spanning from May 16, 2006 up to August, 31, 2006.

In addition, follow hypothesis according to which surface properties of Lybia site is spatially homogeneous and spectral response is temporally stable, reflectance TOA can be compared, especially for multi date observation spanned from May 16, 2006 up to August, 31, 2006.

This hypothesis are obviously rough approximation since, both the atmosphere and the surface have a bidirectional behaviour and both the atmosphere and the surface are not exactly radiometrically over time. But again, for the purpose of a first order assessment of the radiometric stability of the instrument, this method should provide a quality indicator.

Several regions of interest are disseminated over each scene. The regions are located on the area for which the overlapping between consecutive scenes is the most important (fig. 15).

This procedure requires the use of AVNIR-2 band spectral solar irradiance. JAXA provide ESA with these values, they are listed just here after.

Solar spectral Irradiance (w/m² µm)

band1	band2	band3	band4
1943,3	1813,7	1562,3	1076,5

table 12 - AVNIR-2 solar spectral irradiance.

Rescaling gain and offset such as written into product format are listed into table just here below. Please note that rescaling offset is always set to zero value.

File name	Sun elevation (degree)	Rescaling gain - band1	Rescaling gain - band2	Rescaling gain - band3	Rescaling gain - band4
ALAV2A016383020	71,020	0,941	0,914	0,804	0,835
ALAV2A017693040	66,310	0,941	0,914	0,804	0,835
ALAV2A017843010	74,330	0,941	0,914	0,804	0,835
ALAV2A018573000	76,370	0,941	0,914	0,804	0,835
ALAV2A022073010	74,370	0,941	0,914	0,804	0,835
ALAV2A027763000	72,410	0,941	0,914	0,804	0,835
ALAV2A031993000	66,070	0,941	0,914	0,804	0,835

table 13 - Sun elevation and rescaling gain used.

Team

Sebastien Saunier (GAEL Consultant), Richard Santer (LISE).

Working data

Working dataset is the same as the one used for completion of previous verification item (table 11).

Observation date	Scene Id	Pointing angle	DOY
16-mai-06	ALAV2A016383020	0	136
25-mai-06	ALAV2A017693040	-41,5	145
26-mai-06	ALAV2A017843010	21,5	146
31-mai-06	ALAV2A018573000	34,3	151
24-juin-06	ALAV2A022073010	21,5	175
2-août-06	ALAV2A027763000	34,3	214
31-août-06	ALAV2A031993000	34,3	243

table 14 - Dataset used for verification of radiometric calibration stability.

Results

The average TOA reflectance is computed over all regions of interest in each scene and in each spectral band The results are shown in fig. 16 . This figure represents the evolution of the band reflectances along the Day Of Year (DOY). It illustrates the stability of the TOA signal, which can be partially attributed to the stability of the radiometric calibration. Again, this exemplifies to the rough first order the stability of the instrument radiometry.

The results for the observation dated of DOY 145 look inconsistent with regards to the other ones. This is probably due to high pointing angle (-41.5) associated with this acquisition and the resulting increase of signal due to the molecular scattering, decreasing from the blue to the red bands.

When computing standard deviation per band (expressed in percent) and performing basic data interpolation (linear, logarithm, exponential…), we obtained the following results:

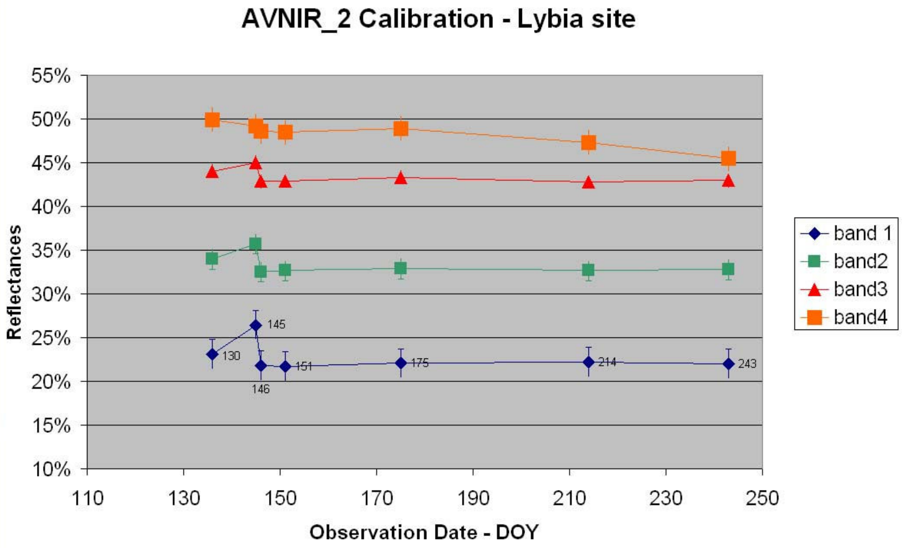

fig. 16 - Reflectance results stability along with observation date.

	band1	band2	band3	band4
standard deviaton (%)	0,49%	0,54%	0,46%	1,53%
slope	-2,4E-05	-4,8E-05	-5,1E-05	-0,00033
R	-0,21	-0,38	-0,46	-0,92

table 15 - Radiometric calibration stability, key results

The standard deviation computed from band number 4 results is slightly upper th an those from other bands.

For the whole of band, a linear interpolation of time series looks the more suitable interpolation method since it gives the best results in term of correlation coefficient.

Results from table 15, tell us that radiometric calibration of AVNIR-2 bands is relatively stable. It is likely that changes of less that 10-20 % in calibration cannot be assessed with this method which does not take into account neither the angular variability of the TOA signal nor the temporal variability of the TOA signal due to day-to-day variations of surface and atmosphere radiometric properties.

5.3 Sensor inter-comparison; Landsat / TM -ALOS / AVNIR-2

Purpose

The main purpose of this exercise is to compare the AVNIR-2 calibration to the TM and ETM+ sensor calibration (respectively on board Landsat 5 and Landsat 7). The purpose of this exercise, again, is not to derive absolute calibration coefficients for AVNIR-2 but rather to get a rough idea of the quality of the AVNIR-2 calibration.

Method

The approach involves comparison of nearly simultaneous TOA radiances over areas observed by the two sensors. For more information on the method and references, please refer to ALOS II optical data verification plan document [R-1].

Team

Gyanesh Chander (SAIC/EROS/USGS).

Working data

Dataset

Following ALOS II/ AVNIR-2 dataset sample, acquired over Libya target zone has been used for band-to-band registration accuracy assessment.

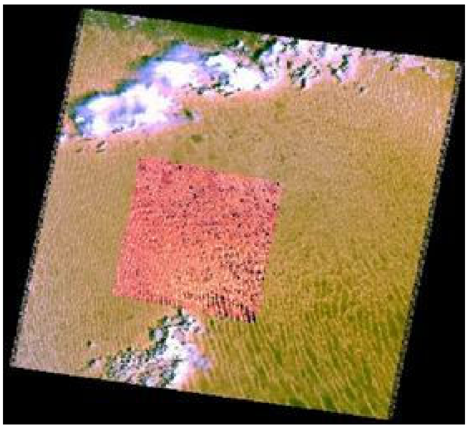

fig. 17 - AVNIR-2 image band composition overlaid TM one.

Observation date	Scene Id	Pointing angle	Path	Sun elevation (degree)
15-mai-06	ALAV2A016383020	-21,5	317	71,02
31-mai-06	ALAV2A018573000	-21,5	317	76,37

table 16 -AVNIR-2 dataset used as working data.

Observation date	Scene Id	Pointing angle (degree)	Path	Sun elevation (degree)
15-mai-06	LT5181040000613510	0	181/40	66,49
31-mai-06	LT5181040000615110	0	181/40	67,557

table 17 - Landsat TM dataset used as reference data.

Spectral response

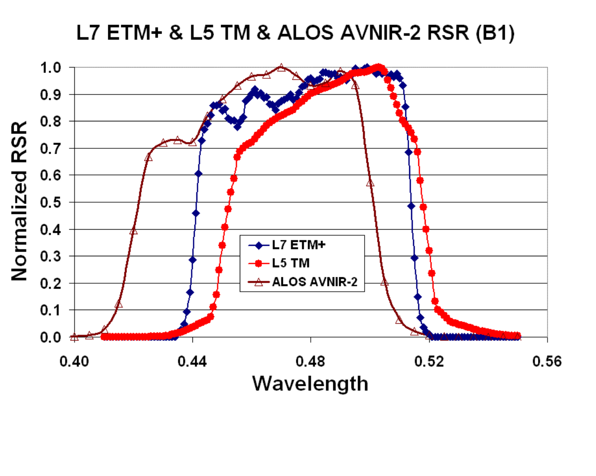

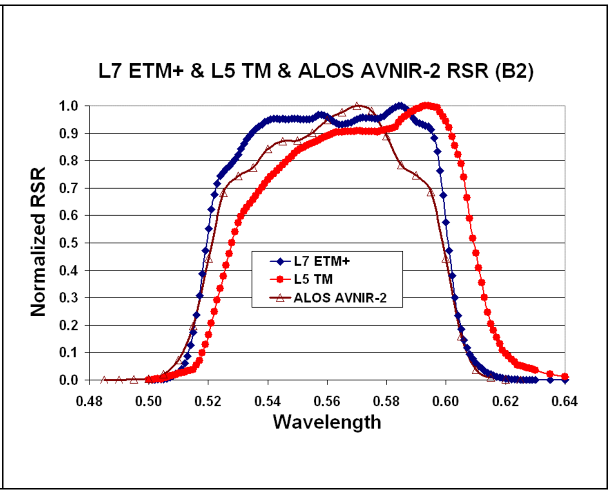

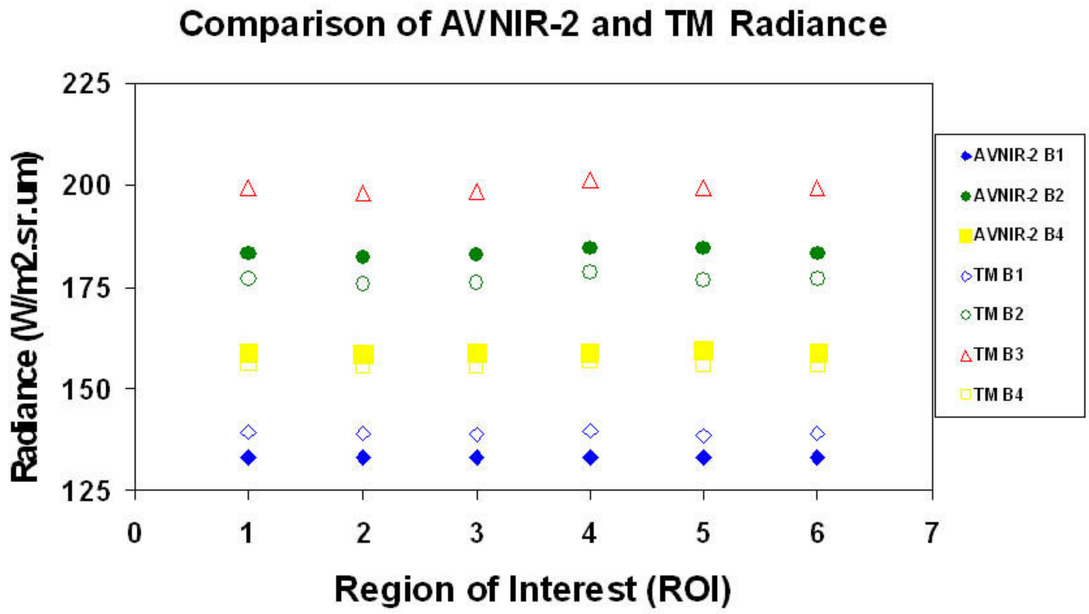

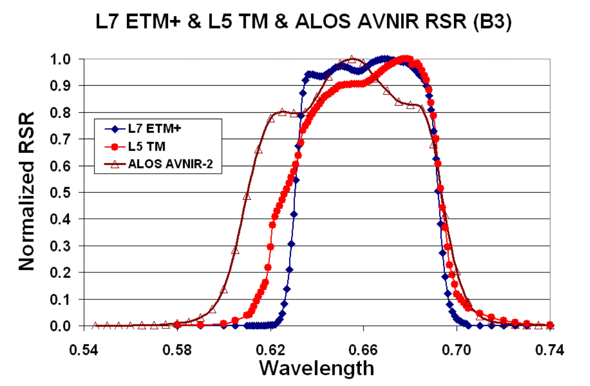

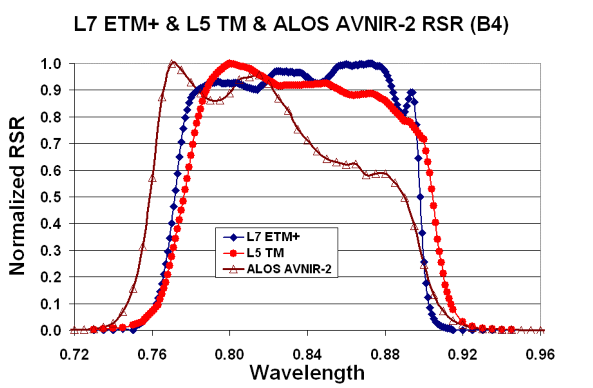

Results

Saturation on AVNIR-2 band 3 makes difficult comparison with TM.

At this time, results reported for this initial cross calibration are focused on one couple of scene (dated of 15 May 2006). The main quantitative conclusions can be summarized as follow:

- AVNIR-2 band 1 TOA radiances are 4% lower than TM ones.
- AVNIR-2 band 2 TOA radiances are 3.7% upper than TM ones.
- AVNIR-2 band 4 TOA radiances are 1.81% upper than TM ones.

The average percent differences in radiance estimates obtained from the ALOS AVNIR-2 agree with those from the L5 TM to within 5%

These values have been tested at one date, over a somewhat peculiar target (Libya) – more dates and sites must be tested to develop more robust relationships. It is difficult to interpret these results directly in terms of calibration differences between LANDSAT TM and AVNIR-2 because the two sensors did not acquire data in bands having identical spectral responses and under identical viewing and illumination geometries. - *Comparison of AVNIR-2 and TM radiance.*

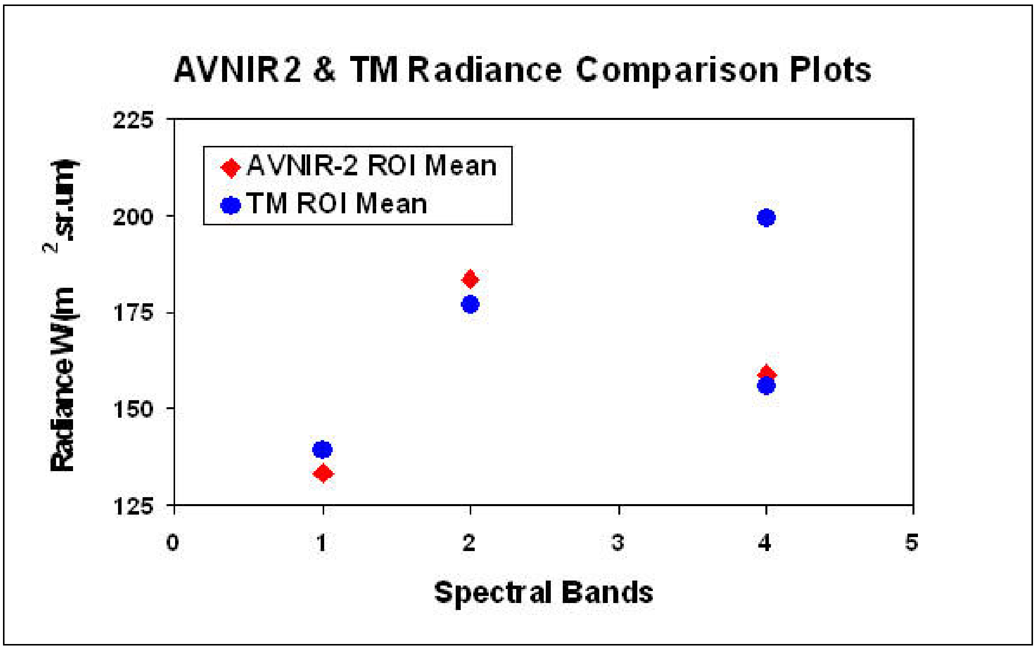

fig. 19 - Comparison of AVNIR-2 and TM radiance along with spectral band.

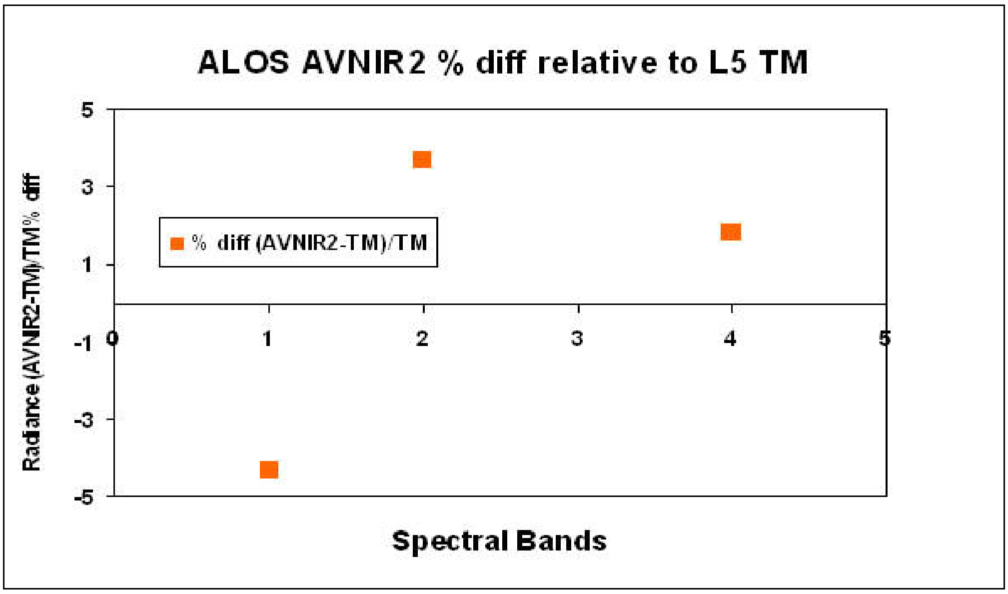

fig. 20 - Comparison of AVNIR-2 and TM radiance along with spectral band.

5.4 Sensor inter-comparison; ENVISAT / MERIS-ALOS / AVNIR-2

Purpose

The purpose of this method is to simulate AVNIR-2 TOA reflectance data in each one of its broad spectral bands, over a Libyan site, and to compare these simulations to the actual AVNIR TOA reflectance measurements.

From the comparison between the simulated TOA reflectances and the actual measurements, we try to assess the quality of the AVNIR-2 calibration.

Method

In order to simulate AVNIR-2 TOA reflectance data, we use what we will refer to as the exogenous satellite data, namely, PARASOL/POLDER, ENVISAT/ MERIS and ENVISAT/AATSR data. The previously listed sensors acquire data over our pre-selected Libyan site on a regular basis. However, the TOA reflectances from theses sensors cannot be directly compared to the AVNIR-2 ones for the following reasons:

- The acquisitions do not occur exactly at the same time: the geometry of illumination of the surface is not the same for exogenous satellite data and AVNIR-2 data.
- The geometry of observation is not the same for all sensors
- The spectral response of the sensors is not the same for all bands.
- The calibration of these

We shall later address later in this section address the question of how to simulate the AVNIR-2 measurements from the exogenous satellite data given all the previously listed limitations forbidding direct comparison between sensors. Let’s first look at the site which was chosen for intercomparison, the exogenous satellite data and why the direct comparison of the exogenous TOA reflectance and AVNIR-2 reflectance over this site cannot give accurate indication on the calibration of the sensor. Further on, we will describe how we can circumvent the limitations of a direct comparison by simulating AVNIR-2 TOA reflectances using the exogenous data.

The Libyan site

The site a desert site made of reddish sand and dunes (see hereafter image). A region of interest was selected that was defined as:

lat_min=-20.16

lat_max=-20.00

long_min=-68.05

long_max=-67.45

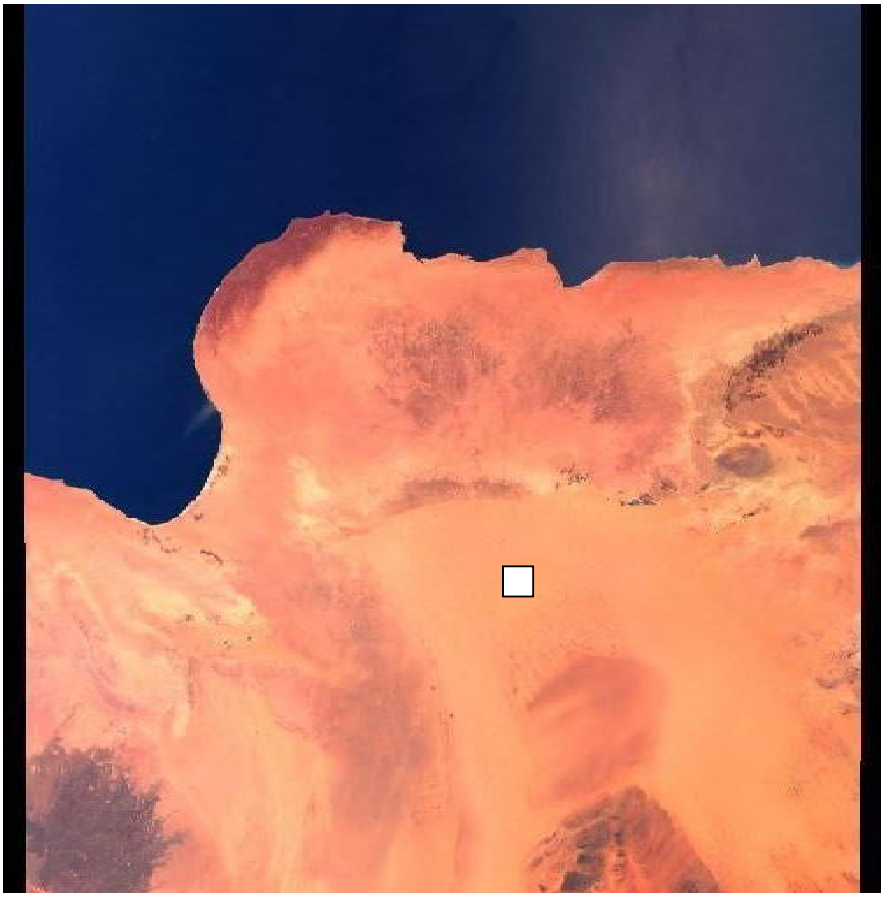

fig. 21 - The Libyan desert site as seen by the ENVISAT/MERIS sensor at 1,2 km resolution. The white square indicate the region of interest over which AVNIR-2, ENVISAT/MERIS, ENVISAT/AATSR and PARASOL/POLDER data where systematically acquired during the first semester of 2006.

Data from the exogenous sensors and AVNIR-2 data where systematically acquired over the site during the first semester of 2006. Here after follow a TOA reflectance spectrum of the region of interest.

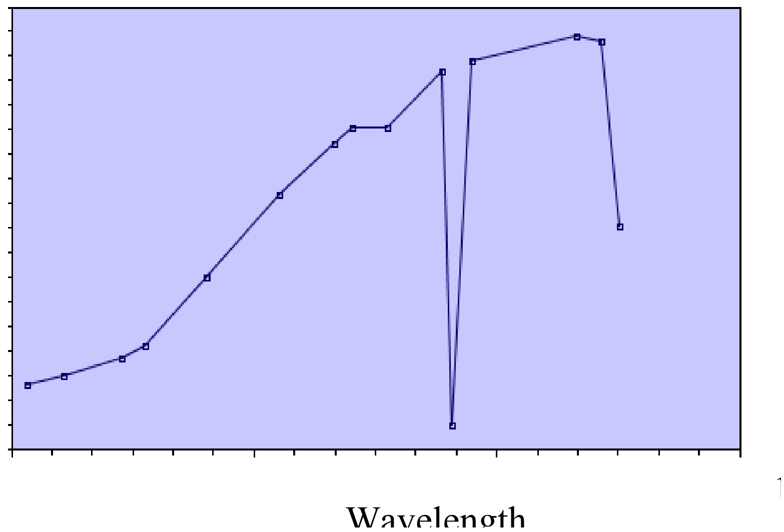

TOA reflectance spectrum extracted in the MERIS 15 spectral bands over the region of interest. Note the deep absorption features in the bands centered at 760 nm and the 900 nm.

If looking at smaller resolution scale (AVNIR-2 resolution) into the data, the typical dune pattern of this desert area appear (see here after figure)

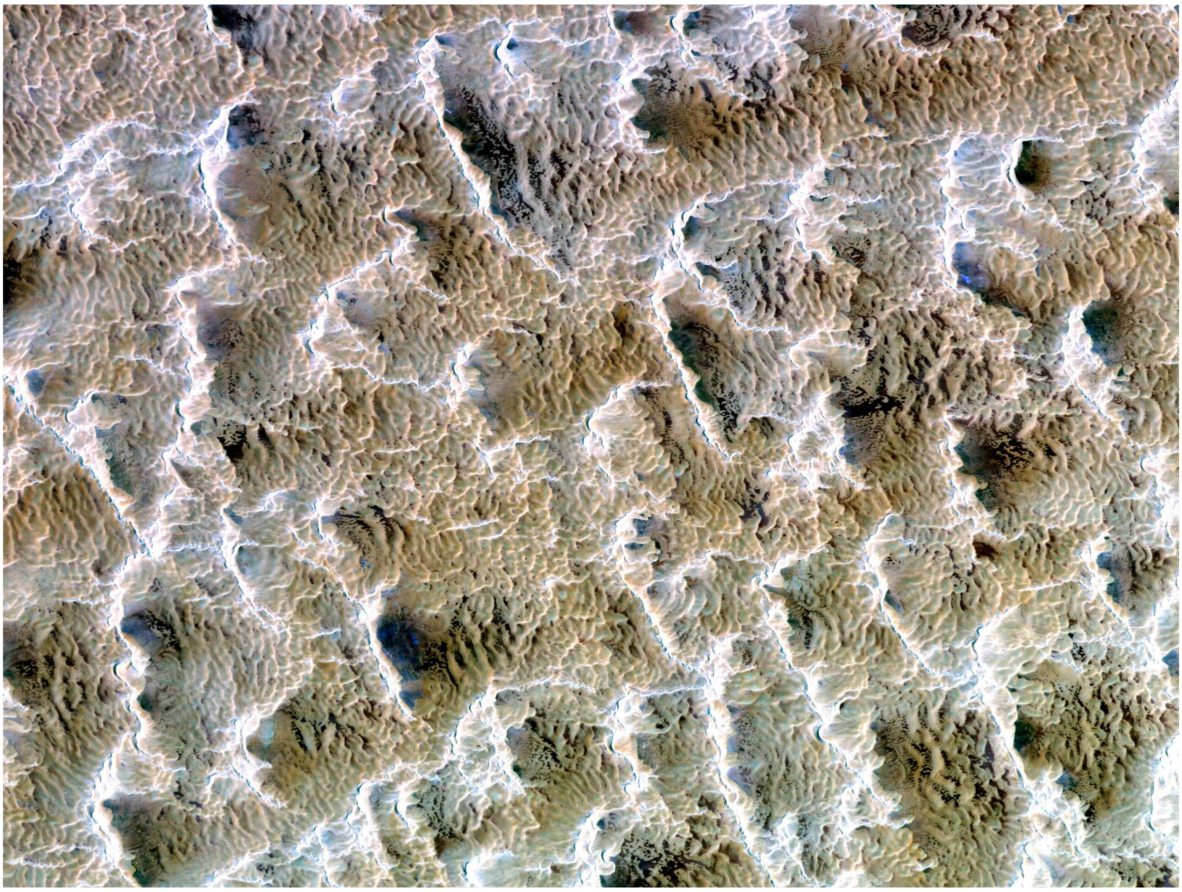

fig. 22 - ALOS / AVNIR-2 true color image over the Libyan site as seen on the 2005/05/16.

The exogenous satellite data: ENVISAT/MERIS, ENVISAT/AATSR and PARASOL/POLDER data

The exogenous data are medium resolution data:

- MERIS: 1.2 km RR
- AATSR: 1 km data
- PARASOL: 6km data

Data were systematically acquired over the site during the periods from:

- January 2006 to August 2006 for MERIS and AATSR
- January 2005 to August 2006 for PARASOL

Type of data extracted:

- L1B TOA radiances

The ALOS data:

Data were downloaded from the Cal/Val portal: www.brockmann-consult.de/CalValPortal

In total 8 acquisitions where carried out during the second quarter of 2006 over the Libyan site and where overlapping the previous indicated region of interest.

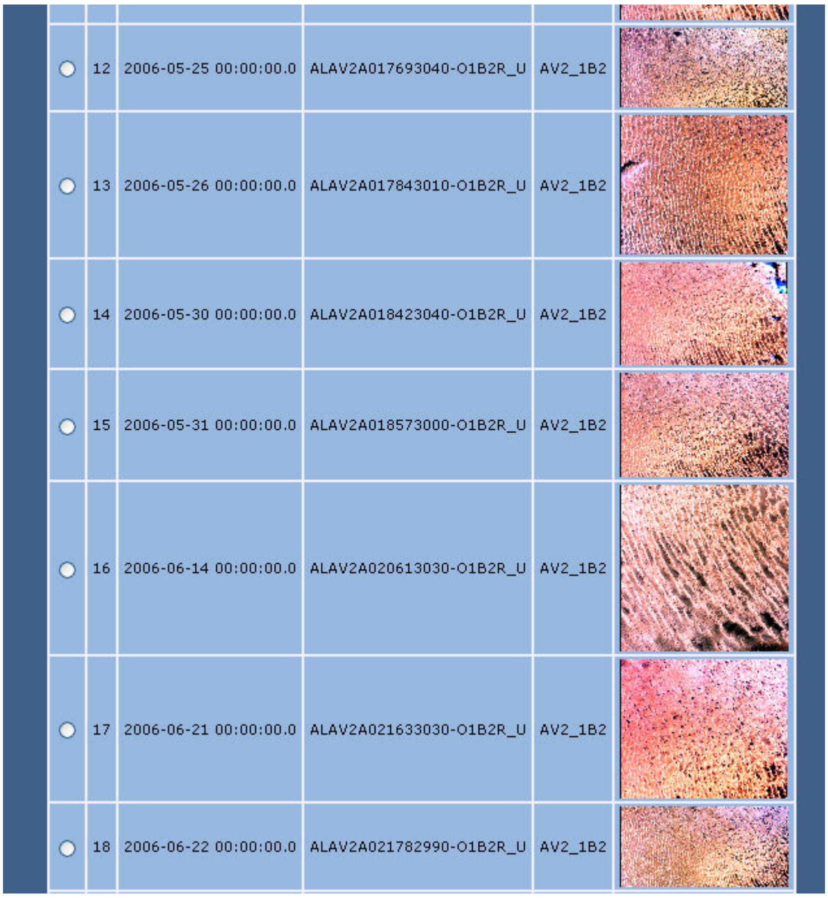

fig. 23 - The Cal/Val portal interface showing the quicklook of the ALOS / AVNIR-2 data.

fig. 24 - The spatial coverage of the 8 acquisitions over the Libya sites. All acquisitions are overlapping.

Direct comparison of the AVNIR-2 acquisition and the exogenous data

In the following analysis all radiance data where converted to reflectance using the sensors spectral response and the Thuillier 2003 irradiance spectrum. As previously mentioned the AVNIR-2 TOA reflectance and the exogenous reflectance data are not directly comparable because the spectral bands of the sensors noticeably differ.

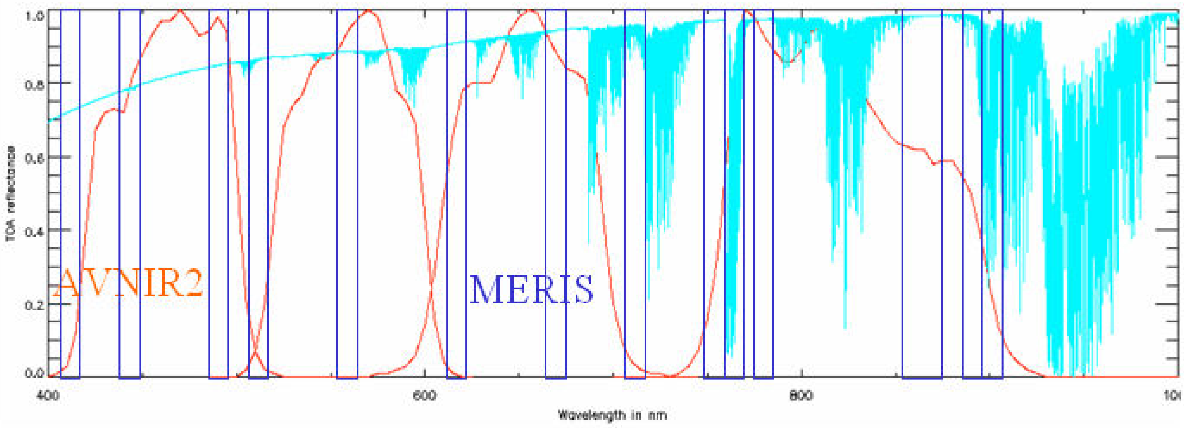

fig. 25 - The AVNIR2 spectral bands (in red) and the atmospheric transmission for an aerosol free, mid latitude summer atmosphere with WV=2 g.m-2 and O3=300 Dobson (in cyan). The MERIS spectral responses are superimposed (in blue).

The broad width of the AVNIR2 spectral bands makes it difficult to compare them directly to the MERIS/AATSR/PARASOL data. Moreover, some of these bands are significantly influenced by atmospheric gaseous absorption of temporally and spatially variable atmospheric constituents: water vapour and ozone. Indeed, the absorption in the AVNIR-2 bands typically reached several percents for band 2, 3 and 4. This absorption induces additional geometrical dependencies in the TOA reflectance angular distribution and also day-to-day variations of the atmospheric inherent reflectance which are measurable at TOA reflectance level.

	410-500	510-600	610-700	750-900
TH20	0.998	0.994	0.993	0.966
TO3	1.000	0.970	0.978	0.999
TO2	1.000	1.000	1.000	0.975
Total downwelling transmission	0.998	0.964	0.971	0.941

Gaseous absorption downward transmission in AVNIR 2 bands for a nadir view, 300 Dobson of O3, 2 g.m-2 of H20 and Psurface=1013.25 Pa and a mid latitude profile.

All previous limitations taken into account, we can however compare MERIS/AATSR/PARASOL bands at 490 nm, 560 nm, 665 nm and 865 nm with respectively band 1, 2, 3 and 4 of AVNIR2 for a first check of the radiometry of the instrument.

We can anticipate differences up to 20 % (??? : educated guess) between AVNIR2 and other the other sensors due to:

- The spectral shape of the reflectance of the target
- The differences in observational geometric conditions
- The influence of absorption by gases in AVNIR2 bands

Larger differences would be suspicious.

Team

Marc Bouvet (ESA / ESTEC)

Working data

The exogenous satellite data: ENVISAT/MERIS, ENVISAT/AATSR and PARASOL/POLDER data

The exogenous data are medium resolution data:

- MERIS: 1.2 km RR
- AATSR: 1 km data
- PARASOL: 6km data

Data were systematically acquired over the site during the periods from:

- January 2006 to August 2006 for MERIS and AATSR
- January 2005 to August 2006 for PARASOL

Type of data extracted:

- L1B TOA radiances

The ALOS data:

Data were downloaded from the Cal/Val portal: www.brockmann-consult.de/CalValPortal

In total 8 acquisitions where carried out during the second quarter of 2006 over the Libyan site and where overlapping the previous indicated region of interest.

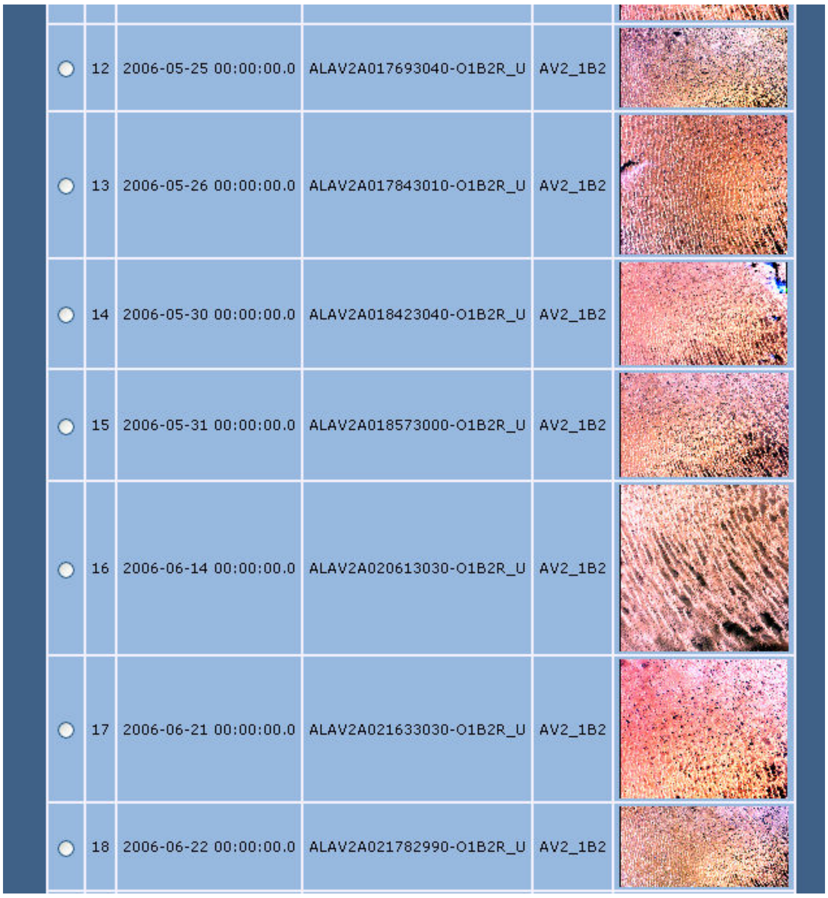

fig. 26 - The Cal/Val portal interface showing the quicklook of the ALOS data.

fig. 27 - The spatial coverage of the 8 acquisitions over the Libya sites. All acquisitions are overlapping.

Results

Direct comparision at TOA reflectance level of the AVNIR-2, MERIS, AATSR and PARASOL data.

When directly looking at TOA reflectance time series of AVNIR-2 band 1, MERIS band 3 and POLDER band 2 (all approximately peaking at 490 nm) we can only draw qualitative conclusions on the calibration of the AVNIR-2 instrument. The TOA reflectance values of AVNIR-2 band 2 lie over the values of MERIS and PARASOL but this could be due to the difference in spectral responses, and illumination/viewing geometries (see next figure).

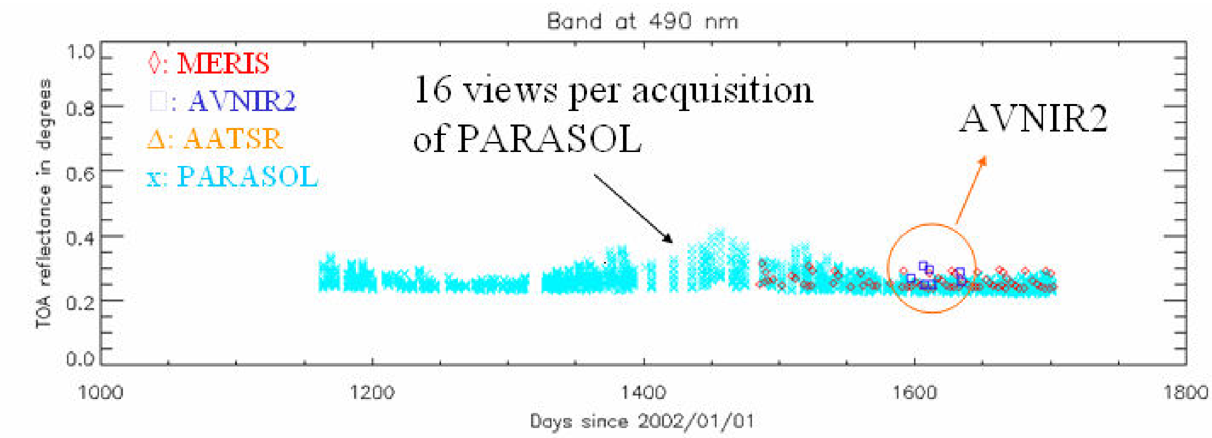

fig. 28 - The MERIS, PARASOL and AVNIR-2 TOA reflectance in respectively band 3, 2 and 1 over the Libyan site.

Similarly is comparing TOA reflectances for MERIS, AATSR and PARASOL

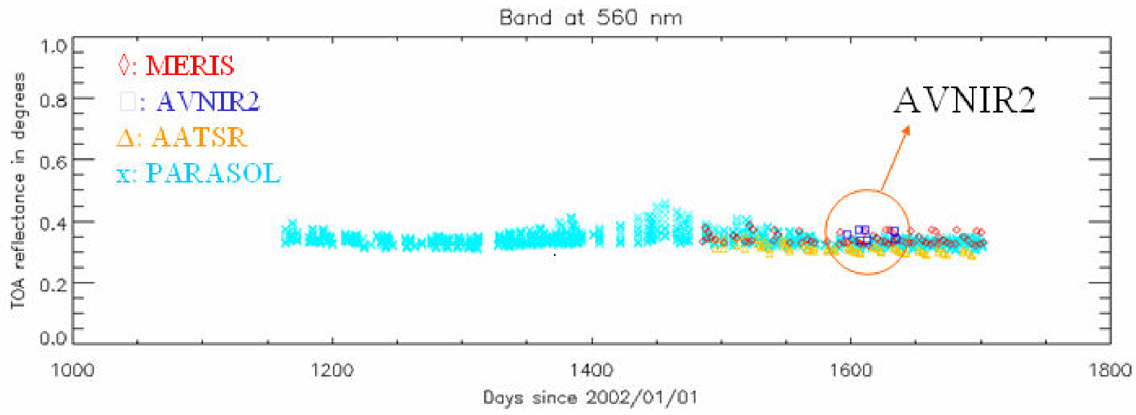

fig. 29 - The MERIS, POLDER, AATSR and AVNIR-2 TOA reflectance in respectively band 5, 4, 1 and 2 over the Libyan site.

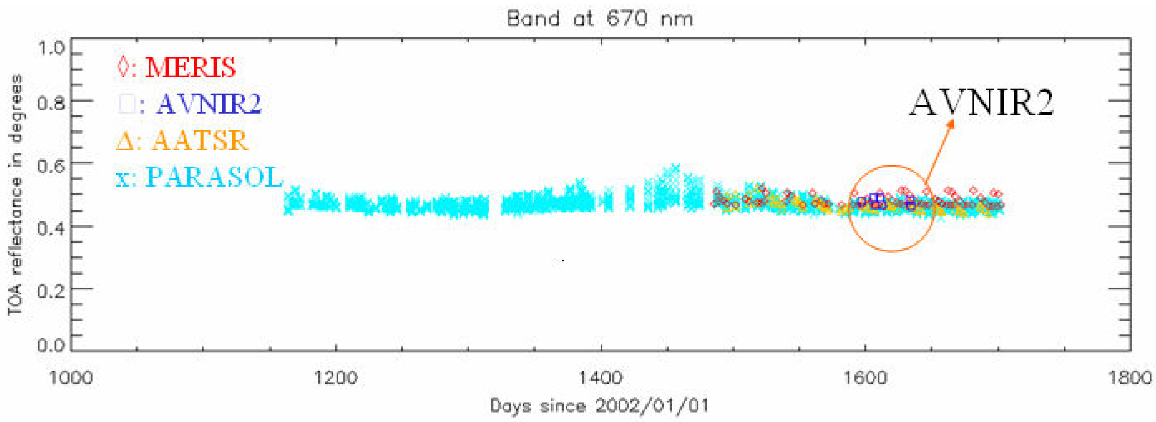

fig. 30 - The MERIS, POLDER, AATSR and AVNIR-2 TOA reflectance in respectively band 7, 5, 2 and 3 over the Libyan site.

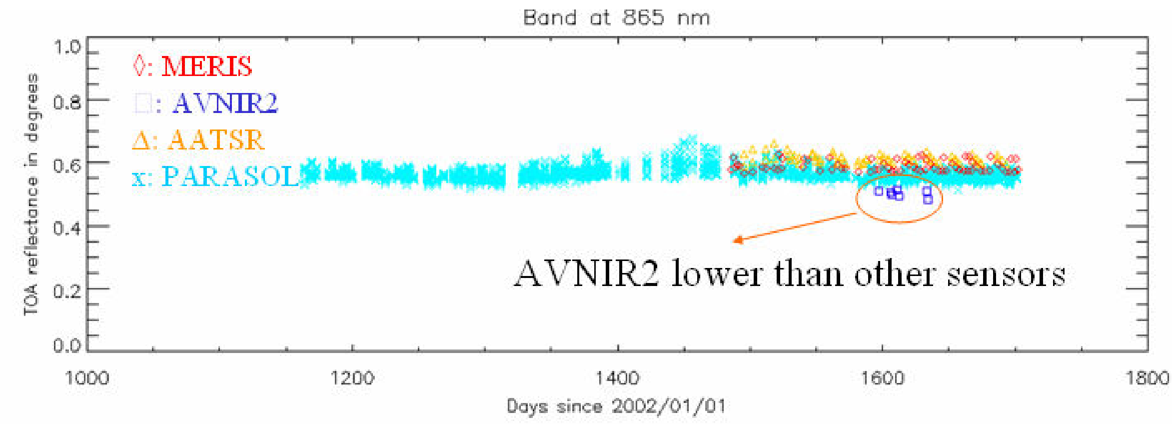

fig. 31 - The MERIS, POLDER, AATSR and AVNIR-2 TOA reflectance in respectively band 13, 8, 3 and 4 over the Libyan site.

In AVNIR-2 band 3, about 50 % of the pixels within the region of interest were saturated as illustrated in the next figure.

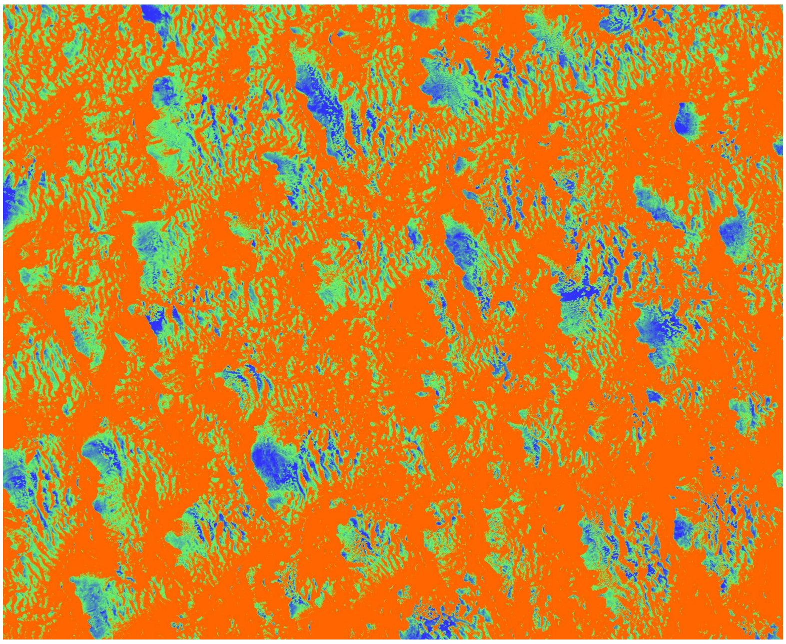

fig. 32 - AVNIR-2 acquisition in band 3 over the Libyan site. Red pixels are saturated.

AVNIR-2 TOA reflectances in band 4 appear to be lower than the TOA reflectances from exogenous sensor narrow bands centered at 860 nm. This could be explained by the significant water vapour and dioxygen absorption present in this band.

As a conclusion of the direct comparison between AVNIR-2 TOA reflectances with the so-called exogenous data we thus can state:

- The direct comparison of AVNIR-2 and exogenous data cannot simply be interpreted in terms of calibration differences because there exist differences between the sensors in terms of viewing geometries, overpass time and the related illumination geometry and last but not least in terms of spectral responses.

- The relatively good agreement (to within 20 %) observed on the time series of TOA reflectances between AVNIR-2 and the exogenous data gives confidence, in a first analysis step, in the calibration of AVNIR-2.

Simulation of the AVNIR-2 TOA reflectance using exogenous data: MERIS, AATSR and PARASOL data.

We have concluded in the previous that it is not straightforward to directly compare AVNIR-2 and the exogenous data because they do not correspond to identical measurements. We hereafter descibe a methodology enabling to partially bridge the gap between AVNIR-2 and exogenous measurements. The general approach is to

1. Intercalibrate exogeneous measurements in comparable spectral bands through the identification of identical/reciprocal observational geometries
2. Radiometrically rescale all exogenous data to the MERIS measurements taken as arbitrary radiometric reference
3. Use radiometricallly rescaled exogenous data to invert the parameters of a BRDF model of the TOA reflectance angular distribution.
4. The BRDF model is then use in forward mode to predict the TOA reflectance in the rescaled exogenous data narrow bands for the AVNIR-2 observational geometry.
5. Spectrally resample the simulated narrow band TOA reflectances for AVNIR-2 observational geometries in the AVNIR-2 spectral bands.

Here follows a sketch of the overall process:

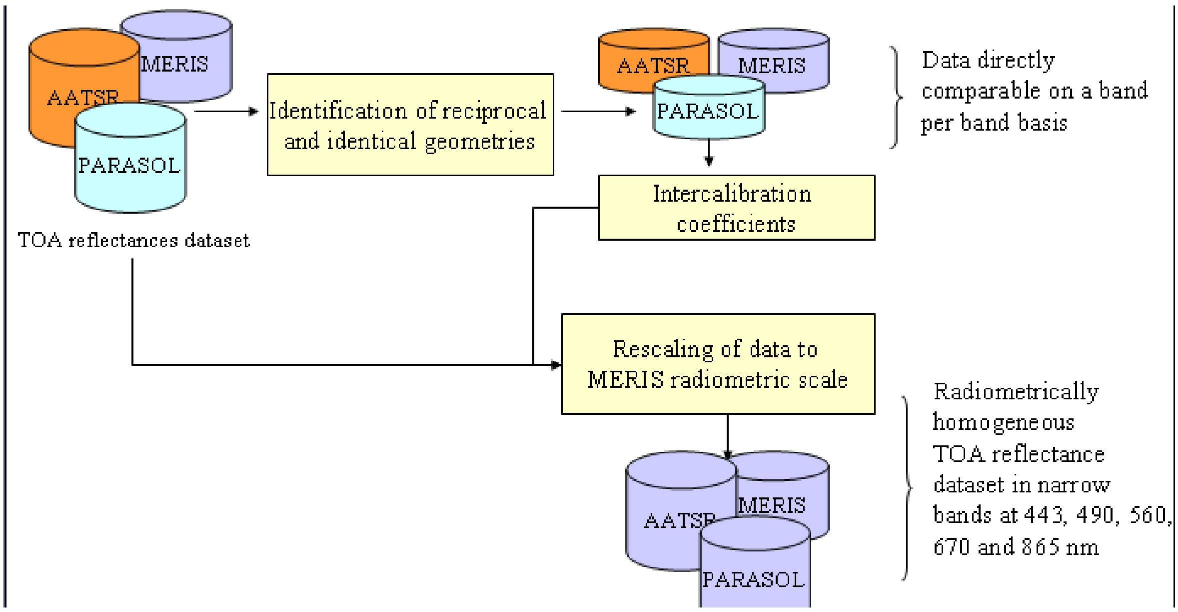

fig. 33 - Part 1 of the approach leading to the simulation of the AVNIR-2 TOA reflectances

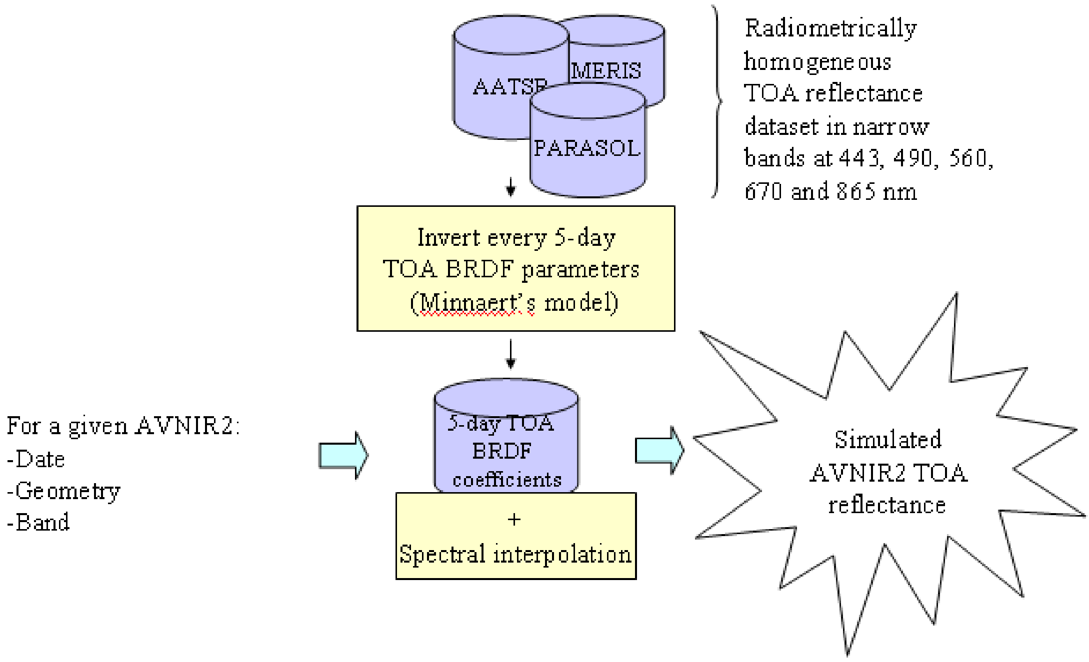

fig. 34 - Part 2 of the approach leading to the simulation of the AVNIR-2 TOA reflectances

To identify reciprocal and identical doublets among the exogenous , doublets between two sensor acquisitions *i* and *j* are searched which have comparable geometries of observation and illumination. To look for such doublets, it is assumed that the TOA reflectance angular distribution obeys a) the principle of reciprocity and b) is symmetrical with respect to the principal plane. The principal of reciprocity states that the following relationship is true:

$$\rho_i^{TOA}\left(SZA_i, VZA_i, RAA_i\right) = \rho_j^{TOA}\left(VZA_j, SZA_j, RAA_j\right) \quad (1)$$

while the symmetrical assumption with respect to the principal plane can be formulated as:

$$\rho_i^{TOA}\left(SZA_i, VZA_i, RAA_i\right) = \rho_j^{TOA}\left(SZA_j, SZA_j, -RAA_j\right) \quad (2)$$

Because an exact geometrical match is often not possible, the search for such geometrical configuration is actually carried out by looking for acquisitions between the sensor *i* and the sensors *j* satisfying the condition $\chi_{ij}<10$ where χ is defined as:

$$\chi_{ij} = \sqrt{\left([SZA_i - SZA_j]^2 + [VZA_i - VZA_j]^2 + \tfrac{1}{4}\left[|RAA_i| - |RAA_j|\right]^2\right)} \quad (3)$$

$\chi_{ij}<10$ roughly corresponds to configurations for which the SZA's, the VZA's do not differ by more than 5° and the RAA's by more than 10°.

Moreover, only doublets of two sensors that satisfy the geometrical criteria of equation (3) and for which the acquisition were performed on the same day or one day apart are kept in the final dataset. This implicitly equivalent to assuming that the TOA reflectance Bidirectional Reflectance Distribution Function (BRDF) does not vary significantly over 24 hours.

Finally, if for a given acquisitions of sensor *i,* there exists several acquisitions from sensor *j* satisfying the previous geometrical and temporal criteria, then only the matching acquisition from sensor *j* for which the χ_{ij} is the smallest is kept to form a doublet with the acquisition of sensor *i*.

The results of the identification of identical and reciprocal geometries among the exogenous dataset leads to time series for each spectral band where the exogenous sensors spectral responses overlap (see next figure).

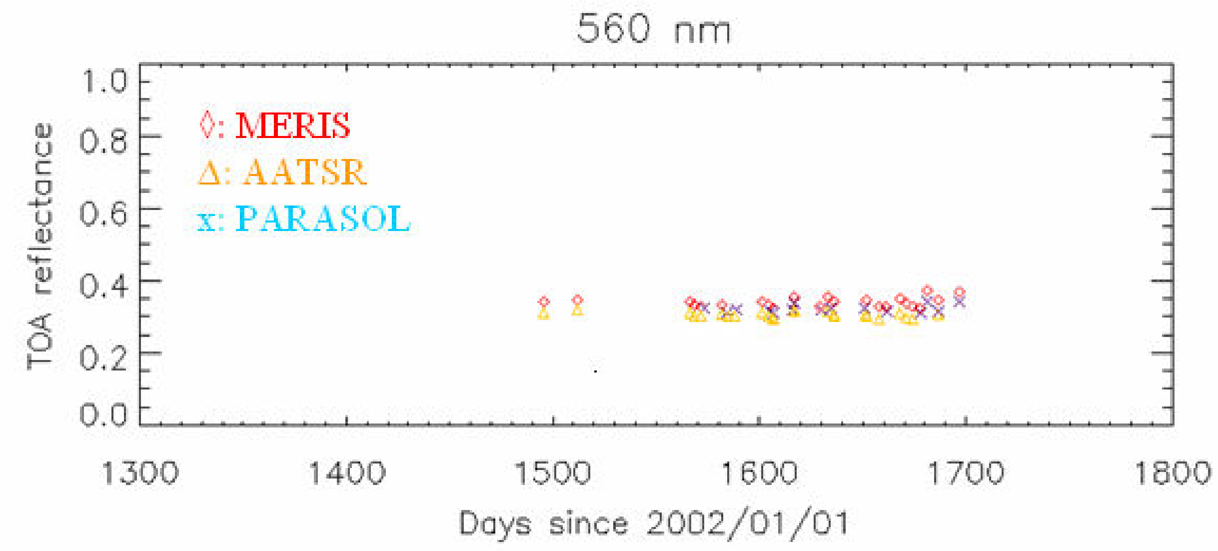

fig. 35 - The time series of MERIS, AATSR and PARASOL data after the screening for identical and reciprocal geometries in the common band 560 nm.

The next figure shows the relative difference between two sensors TOA reflectances observation.

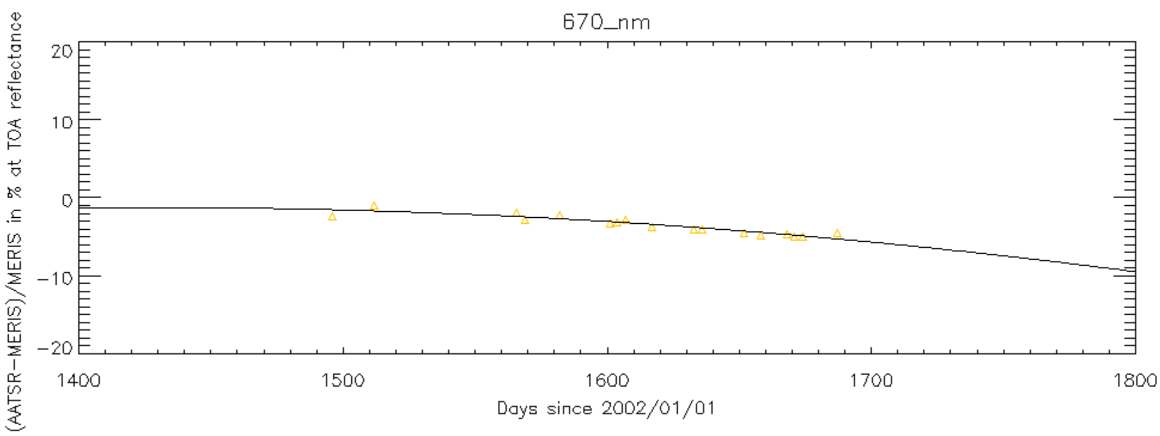

fig. 36 - The relative difference in % between the TOA reflectances of AATSR and MERIS (MERIS being taken as arbitrary reference) is shown in yellow triangles. The black like shows a least square fit of the data.

Least square fits between AATSR-MERIS, PARASOL-MERIS, with a second order polynomial for the bands at 440 nm, 490 nm, 560nm, 670, 870nm are obtained. They enable to rescale PARASOL and AATSR TOA reflectances in the previous bands on MERIS radiometric scale. It is an Intercalibration process which is well justified since the spectral bands of the MERIS, AATSR and PARASOL bands are very similar and the geometries of observation have been chosen to be identical and reciprocal.

We can however apply the Intercalibration to all exogenous data, includind the non-reciprocal and no-identical doublets. We now possess a radiometrically coherent dataset. All observation from the exogenous dataset are binned temporally every 5 days and are used to invert a Minnaert BRDF model (see reference). Following *Minnaert 1941* we can write:

$$\rho^{TOA}(\theta_s,\theta_v) = \rho_0 \frac{k+1}{2}(\cos\theta_s \cos\theta_s)$$

The parameters k and ρ_0 are inverted every 5 days (see here after figure for a plot of the data).

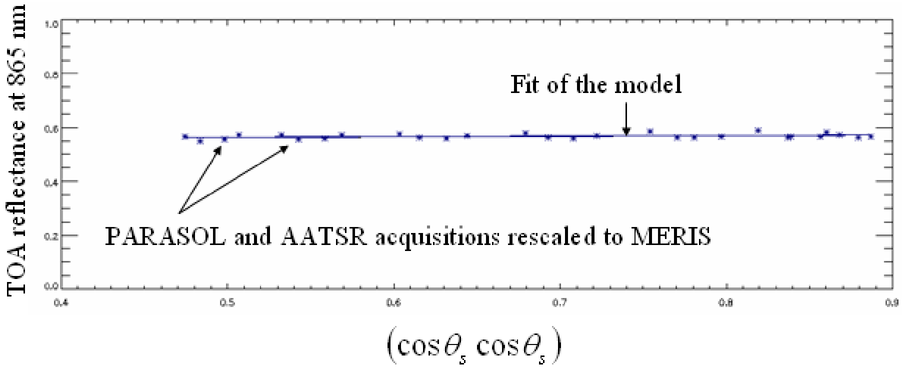

fig. 37 - All MERIS, AATSR, PARASOL data rescaled radiometrically to MERIS radiometric scale are plotted against the cosine of the sun zenith angle and the viewing zenith angle and show a good fit to the Minnaert's BRDF model.

The BRDF model is then run in forward mode and provides TOA reflectances in narrow bands (440 nm, 490 nm, 560nm, 670, 870nm) for the AVNIR-2 geometry of observation. Using the AVNIR-2 spectral responses, we can generate AVNIR-2 like observations (see figure here after)

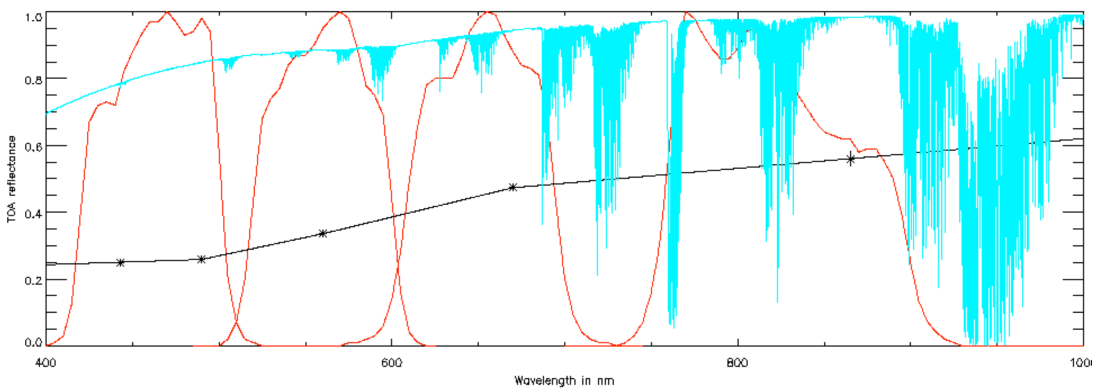

fig. 38 - For a given observation, the TOA reflectance in narrow bands (black stars) is simulated in the AVNIR-2 geometries. The black like is the linear interpolation of these simulated TOA reflectances. In red, the spectral response of the AVNIR-2 sensor. In cyan, the atmospheric transmission for an aerosol free, mid latitude summer atmosphere with WV=2 g.m-2 and O3=300 Dobson

However, the simple convolution of the linearly interpolated TOA reflectance spectrum (obtained from the exogenous dataset and the Minnaert BRDF model) with the AVNIR lead to results that are not directly comparable to the AVNIR-2 observations. Indeed, as shown in the previous figure, the atmospheric absorption in AVNIR-2 bands is significant and can only be assess using in situ atmospheric data. While interpolating the narrow bands, we do not take this effect into account and this should be kept in mind while comparing simulated AVNIR-2 data to actual AVNIR-2 data.

If we look at the following relative error (in %)

$$\frac{\left[\rho^{TOA}_{AVNIR2}\right]_{measured} - \left[\rho^{TOA}_{AVNIR2}\right]_{predicted}}{\left[\rho^{TOA}_{AVNIR2}\right]_{predicted}}$$

We obtain:

	Acquisition 1	Acquisition 2	Acquisition 3	Acquisition 4	Acquisition 5	Acquisition 6	Acquisition 7	Average
Band 1	10.3 %	23.1 %	7.6 %	18.7 %	0.7 %	21.8 %	1.2 %	11.9 %
Band 2	5.4 %	14.1 %	3.8 %	10.5 %	0.9 %	10.7 %	0.9 %	6.6 %
Band 3	6.3 %	12.8 %	6.5 %	9.4 %	4.2 %	8.4 %	3.2 %	7.2 %
Band 4	-6.5 %	-4.3 %	-6.5 %	-4.4 %	-8.3 %	-6.2 %	-10.5 %	-6.7 %

To interpret these results, we should remember that:

- Band 3 and 4 contains strong H2O and O2 signature which cannot be modelled accurately with a simple linear interpolation of the narrow band reflectance predicted with the TOA BRDF model
- Band 3 is saturated
- Band 1 and 2 are in region of the spectrum where a linear interpolation of the narrow band reflectance predicted with the TOA BRDF model could be good enough.

The strong variability on a date to data basis in particular for band 1 is suspicious. A possible explanation is that we used as a proxi for the viewing azimuth angle the so-called ‘orientation angles’ +90 degrees when the incident angle was ‘right’ and the ‘orientation angles’ -90 degrees when the incident angle was ‘left’.

The value of the viewing azimuth angle remains an issue.

References:

Minnaert, M. .The Reciprocity Principle in Lunar Photometry,. *Astrophysical Journal*, Vol. 93, 1941.

Thuillier, G., M. Hersé, P. C. Simon, D. Labs, H. Mandel, D. Gillotay, and T. Foujols, 2003, "The solar spectral irradiance from 200 to 2400 nm as measured by the SOLSPEC spectrometer from the ATLAS 1-2-3 and EURECA missions, *Solar Physics*, 214(1): 1-22.